2018-11-01

Repair and Adaptation of Aged Skeletal Muscle to Nonpathological Muscle Damage: The Influence of Macrophage Polarization

Jacob R. Sorensen
Brigham Young University

Repair and Adaptation of Aged Skeletal Muscle to Nonpathological Muscle Damage: The Influence of Macrophage Polarization

Jacob R. Sorensen

A dissertation submitted to the faculty of
Brigham Young University
in partial fulfillment of the requirements for the degree of

Doctor of Philosophy

Allen Parcell, Chair
Robert Hyldahl
Gary Mack
David Thomson
J. Ty Hopkins

Department of Exercise Sciences

Brigham Young University

ABSTRACT
Repair and Adaptation of Aged Skeletal Muscle to Nonpathological Muscle Damage: The Influence of Macrophage Polarization

Jacob R. Sorensen
Department of Exercise Sciences, BYU
Doctor of Philosophy

The age-related loss of skeletal muscle mass and function is accompanied by a decline in regenerative capacity. The processes that facilitate healthy muscle repair are complex, involving several phases of degradation and rebuilding of muscle tissue and the surrounding microenvironment. Specifically, myogenic progenitor cells known as satellite cells are the most influential in repairing damaged muscle tissue. Following injury, satellite cells become activated and migrate, proliferate and fuse with mature skeletal muscle fibers to restore homeostasis to the tissue. However, satellite cells do not act in isolation, a robust inflammatory response is necessary to facilitate successful and rapid healing. Macrophages are one of the first and most abundant immune cells to infiltrate damaged skeletal muscle tissue. Primarily, macrophages adapt to a proinflammatory state to clear the area of cellular debris, promote degradation of the extracellular matrix and stimulate satellite cell activation and proliferation. Afterwards, a timely transition to an anti-inflammatory state directs rebuilding of the extracellular matrix and terminal differentiation of satellite cells. Indeed, the inhibition of macrophage activity leads to impaired healing and loss of skeletal muscle function. Little is known regarding the behavior of macrophages in aged skeletal muscle following injury in humans. Thus, the objective of this dissertation is to investigate the age-related response of macrophages in human skeletal muscle, and their role in muscle repair.

Keywords: satellite cells, macrophage, inflammation, exercise-induced muscle damage, extracellular matrix

ACKNOWLEDGEMENTS

I would first like to acknowledge Dr. Robert Hyldahl. You have been an incredible advisor. You have worked to provide me with every opportunity to grow as a scientist, academic, and person. You have been committed, attentive and involved in my work, and I hope that I can be a leader like you in my own career. Thank you.

To my dissertation committee: Thank you for generously giving your time and feedback, especially on short notice at times. Your contributions have enriched my experience as a doctoral student.

Thank you to Maggie Shibla and Barb Hehl. You both have been a wealth of knowledge and have been very helpful to me in the pursuit of my PhD. Thank you for all of your time, patience, and interest in my life.

Thank you to my fellow lab members: Nani, Alex and Kyle for your willingness to take on new projects and your dedication to our success. Also, Paul and Mike for your insight and help throughout our four wonderful years together. It has been a fun and cherished time, I owe so much of my success to you all.

My success comes from the help and sacrifice of family and friends. To Kathleen DeGraaff for letting us share your life for the past four years. To Kent and Jill Sorensen and other siblings for caring for our kids, especially those fun Tuesdays in the yard. Thank you all for your support and love.

Most of all, I would like to thank my incredible wife, Summer, and our four wonderful children: Dre, Kalia, Jet, and Dru. Thank you for your continued love, support and dedication. I look forward to the family adventures that lie ahead and the memories we will make together. Thank you for being the greatest part of my life. I love you all so much.

TABLE OF CONTENTS

LIST OF TABLES

LIST OF FIGURES

INTRODUCTION

Humans age on two different scales: chronologically and biologically. Chronological age refers to the amount of time (years) a person has lived, while biological age refers to how old a person seems, taking many lifestyle factors into consideration (eg, diet, exercise, stress, smoking, medications and sleeping habits). It is widely held that participation in regular physical activity can drastically reduce the rate of biological aging (1). Nonetheless, whether early or late, we each succumb to the effects of biological decay. A hallmark of biological aging is the loss of skeletal muscle mass, replaced by the infiltration of fatty and fibrotic tissue. This decline in muscle quality is followed by an exacerbated reduction of muscle functional capacity, and the inability to adapt appropriately to stress. As such, the prevalence and duration of injury increases with advancing age and results in greater incidence of disease (eg, heart disease and diabetes) (2). Furthermore, with the rising age of the general population, the complications of aging present a major obstacle for the healthcare industry, coupled with increased financial demands on the economy (3-6). Thus, the mechanisms that govern healthy muscle adaptation, coupled with an appreciative knowledge of the changes that transpire in skeletal muscle with advancing age, warrant a greater understanding of the treatment and development of interventions that would provide immediate clinical value to the aging population.

The rather remarkable capacity of healthy skeletal muscle to repair following injury is attributed to a specialized cell known as a satellite cell. Appropriately named, the unique sublaminar location of satellite cells allows constant monitoring of muscle fiber health, while facilitating interactions within the extracellular environment. Studies indicate that repair following injury, and maintenance of skeletal muscle mass, is vitally dependent on a healthy and active pool of satellite cells (7). However, satellite cells do not work in isolation. A complex and

transient transition occurs within the extracellular environment following stress, which directs satellite cell behavior. Most notable is the rapid and robust infiltration and activation of immune cells, in particular, the macrophage (8).

Macrophages are one of the first and most abundant immune cells to arrive at the site of damage. Macrophages clear debris, release extracellular matrix degrading enzymes and direct satellite cell behavior by secreting cytokines and growth factors (9). Indeed, damaged muscle tissue fails to heal when macrophage infiltration is attenuated (10). However, recent studies suggest that in addition to macrophage infiltration, their capacity to transition between proinflammatory and anti-inflammatory functions (ie, their polarization) is also critical for healthy healing and retention of muscle quality (11). Along this line, aging is associated with a gradual deterioration of the immune system, known as immunosenescence. It involves a declined capacity to fight off infections and develop long-term immune memory, especially by vaccination (12). However, it is not clear whether immunosenescence would impact healing of skeletal muscle tissue in the elderly. Therefore, an unexplored possibility is that impaired healing of aged skeletal muscle is in part due to a dysfunctional immune response. One study that supports this hypothesis found that infiltrating macrophages in old human muscle following a bout of resistance exercise displayed a greater proportion of anti-inflammatory macrophages relative to the young, which was coupled to dysregulated cytokine concentrations in the muscle tissue (13). Likewise, we recently showed that several proinflammatory and anti-inflammatory cytokines were dysregulated in young and old subjects following a bout of exercise-induced muscle damage (14). Most interesting was the early activation of the TGF-beta signaling pathway, which is largely influenced by the activity of anti-inflammatory macrophages. Taken together, these findings suggest that aged macrophages may be unable to mount an appropriate

proinflammatory response, resulting in a premature or untimely transition to a proregenerative phenotype that ultimately attenuates transient changes in the extracellular environment and limits satellite cell activity. In other words, just as the aging immune system is less capable of fighting off infection, so, too, is its ability to mount an appropriate inflammatory response to heal damaged muscle tissue.

Therefore, the purpose of this dissertation project is to test the overall hypothesis that a dysfunctional immune system is in part responsible for the age-related decline in skeletal muscle repair and adaptation. To address this hypothesis in humans, we have employed a model whereby we are able to transiently damage the skeletal muscle via the application of repeated lengthening (eccentric) contractions. This protocol has been shown to induce a reproducible damage/repair cycle that is characterized by extensive inflammatory cell infiltration and subsequent muscle adaptation (15, 16). Study I presents a broad assessment of the acute changes that take place in the extracellular environment of young and old humans following this form of muscle damage. Study II more specifically investigates the details related to macrophage infiltration and activation in young and old subjects in response to damage. Additionally, Study II uses a more mechanistic tissue culture approach to further test the hypothesis that the functional capacity of old immune cells (macrophages) declines with age and, as a result, has negative implications for satellite cell activation.

AIMS AND HYPOTHESES

Study I: Acute Extracellular Matrix, Inflammatory and MAPK Response to Lengthening Contractions in Elderly Human Skeletal Muscle

Published: *Exp Gerontol.* 2018 Jun;106:28-38. doi: 10.1016/j.exger.2018.02.013.

Statement of the Problem

There exists an age-related loss of reparative potential in human skeletal muscle. Successful repair in young individuals is characterized by satellite cell activation, extracellular matrix remodeling, and an increased and time-dependent inflammatory response. These responses have mostly been described in animal models with extreme damaging stimuli. Therefore, the purpose of the study was to investigate these acute responses to damage in older humans using an eccentric muscle damaging model.

Specific Aim 1

To induce skeletal muscle damage and examine the functional recovery of the knee extensor muscles in young and old adults.

Hypothesis 1

The bout of 300 eccentric contractions will induce muscle soreness and declines of muscle strength—indirect measures of muscle damage. However, the recovery of strength will be delayed in the old.

Study Design

Eleven young (aged 22 ± 2 yrs) and 8 older (aged 71 ± 7 yrs) subjects performed 300 eccentric (lengthening) contractions (30 sets of 10 repetitions) on a Biodex dynamometer. Work, power, and torque measures were collected and averaged for each set. Muscle soreness and functional strength, power (60º and 180º • sec isokinetic) and impulse (70º isometric) measures were taken prior to and immediately, 24 and 72 hours following the exercise as an indirect measure of skeletal muscle damage.

Brief Results

The 11 young (aged 22 ± 2 yrs) and 8 older (aged 71 ± 7 yrs) subjects performed a similar amount of total work during the exercise bout of 300 lengthening contractions. However, the older subjects showed a greater resistance to fatigue through the exercise protocol, indicated by a preservation of average torque output throughout the 30 sets of eccentric contractions (group x time, $p = 0.038$). Furthermore, both groups experienced a significant increase in muscle soreness and a decrease in strength, power, and impulse. The loss of strength was markedly greater in the young. Nonetheless, both young and old subjects demonstrated a similar recovery response, but due to the greater overall force loss in the young, the return to baseline strength was not observed by 72 hours following the exercise.

Specific Aim 2

To examine the acute response of extracellular matrix, inflammatory cytokines and MAPK signaling events in young (18 to 30 yrs) and old (65+ yrs) skeletal muscle following a bout of exercise-induced muscle damage.

Hypothesis 2

The appearance of a "transitional matrix" will be blunted in old skeletal muscle, coupled with a premature activation of signaling pathways that contribute to extracellular matrix rebuilding. Furthermore, inflammation will generally be elevated in the old and have an atypical response when compared to the young following the exercise. Lastly, members of the stress related MAPK signaling pathway will be greater in the old when compared to the young following the exercise protocol.

Brief Methods

The 11 young (22 ± 2 yrs) and 8 old (71 ± 7 yrs) subjects performed 300 eccentric (lengthening) contractions (30 sets of 10 repetitions) on a Biodex dynamometer. Muscle biopsies were collected prior to and at 3, 24, and 72 hours postexercise and used for immunohistological analysis of extracellular matrix proteins and multiplexing bead assays for cell signaling pathways and inflammatory markers.

Brief Results

As hypothesized, immunohistological examination of proteins that contribute to the "transitional extracellular matrix" increased in young subjects by 24 or 72 hours following the muscle damaging exercise. Conversely, some, but not all, of the measured proteins were unchanged in aged muscle.

Multiplexing analysis of protein homogenates showed that the overall expression of TGF-βRII and SMAD3 protein concentrations were elevated by 72 hours postexercise in both young and old subjects. However, the overall expression was greater in the old, with a trend for premature activation by 24 hours postexercise in the old, but not the young.

Surprisingly, baseline inflammatory markers were similar between young and old subjects for all measurable markers. However, following the exercise, 8 of the 13 measured biomarkers changed among both young and old subjects. Nonetheless, there was a marked dysregulation in several inflammatory markers between young and old, which included: greater overall expression of CCL2 (MCP-1), and IL-8, with a decreased overall expression of IL-1b, and a group × time interaction for NF-κB activity.

Lastly, there was a rapid and robust increase in both the p38 and JNK proteins in the old at 3 hours postexercise, before they returned to baseline values. No response was measured in the young (group × time, $p < 0.05$).

Study IIa: A Time Course Characterization of Skeletal Muscle Macrophage Infiltration and Polarization Following Damaging Contractions in Young and Old Humans

Statement of the Problem

Macrophages are known to play an important role in directing muscle repair of damaged tissue, specifically by undergoing a timely transition from an early M1 proinflammatory to a later M2 anti-inflammatory, proregenerative phenotype. Animal studies suggest that with age, macrophage polarity is dysregulated (11, 13, 17), yet it is not known whether macrophages prematurely transition to an M2 phenotype during repair of elderly human skeletal muscle.

Specific Aim 1

Implement an acute time course characterization of macrophage infiltration and activation prior to and out to 72 hours after the bout of muscle-damaging lengthening contractions in young (18 to 30 yrs) and old (65+ yrs) individuals.

Hypothesis 1

A greater proportion of macrophages in old skeletal muscle will stain positive for the cell surface marker CD206, representative of the M2 anti-inflammatory phenotype, relative to the proportion of M2 macrophages in young muscle.

Study Design

Eleven young (aged 22 ± 2 yrs, n = 11) and 8 older (aged 71 ± 7 yrs, n = 8) male and female adults performed an intense exercise bout consisting of 300 eccentric lengthening contractions at an angular velocity of 60° sec^{-1} on a Biodex dynamometer to induce acute muscle

damage. Percutaneous needle biopsies were taken from the vastus lateralis muscle prior to and at 3, 24, and 72 hours following the bout of lengthening contractions. Muscle biopsy samples were mounted, frozen, and sectioned for immunohistological analysis of macrophage activity.

Brief Results

As hypothesized, there was a significantly greater proportion of M2-like macrophages across all time points for the older relative to the younger subjects (group: $p = 0.0037$). Furthermore, the older subjects demonstrated a reduced capacity to mount a strong M1 proinflammatory response relative to the young. This was demonstrated in the reduced proportion of M1-like macrophages at 24 hours postexercise (young: $75 \pm 15\%$ vs old: $53 \pm 18\%$, $p = 0.027$).

Study IIb: Examination of the Capacity of Young and Old Macrophages to Transition to a Proinflammatory or Anti-Inflammatory Phenotype and Influence Myoblast Activity

Statement of the Problem

Studies performed using young and old parabiosis in animals showed a restoration of old skeletal muscle function and satellite cell activation to a youthfullike state (18), suggesting that something in the systemic circulation is partly responsible for the age-related decline of skeletal muscles regenerative capacity. In support of this notion, a recent study by Wang et al. shows that satellite cells transition to a fibroblastlike phenotype with advancing age of the immune system (19). Therefore, as immune cells are vital to successful muscle repair, and have been shown to be dysfunctional in fighting infection in the elderly, it stands to reason that they would be a source of dysfunction in regenerating muscle of the elderly. In fact, the previous findings suggest that macrophages are abnormal in the muscle of older individuals (14). Specifically, we found that aged macrophages appear less capable of mounting a proinflammatory response following

muscle damaging exercise and are more likely to take on an anti-inflammatory phenotype. Indeed, animal studies have demonstrated that aged macrophages display dysfunctional characteristics in skeletal muscle with advancing age (17). Yet, studies that investigate immune cell function related to human skeletal muscle are lacking.

Specific Aim 1a

To test the sensitivity of young (18 to 30 yrs) and old (65+ yrs) macrophages to adapt to a proinflammatory or anti-inflammatory phenotype following treatment with polarizing cytokines.

Hypothesis 1a

Old macrophages will display increased sensitivity to anti-inflammatory cytokines, while being less likely to respond to proinflammatory treatments.

Specific Aim 1b

Test whether old (65+ yrs) macrophages express a dysregulated assortment of proinflammatory and anti-inflammatory cytokines in relation to young (18 to 30 yrs) macrophages.

Hypothesis 1b

Macrophages from old subjects will secrete a greater proportion of anti-inflammatory cytokines relative to young macrophages.

Specific Aim 2

Test the impact of young (18 to 30 yrs) and old (65+ yrs) macrophage-conditioned medium on the proliferation and differentiation potential of human primary myoblasts.

Hypothesis 2

Aged myoblasts will demonstrate increased proliferation and differentiation potential when grown in young macrophage-conditioned medium.

Study Design

Five young (24.6 ± 3.6) and 5 old (75.2 ± 3.6) subjects were recruited to the lab for a 70-mL blood draw. Monocytes were isolated from young and old human blood draws and differentiated into macrophages (20). Following 6 days of macrophage maturation, cells were suspended in proinflammatory or anti-inflammatory polarizing cytokine medium for 24 hours. Following 24 hours of incubation, cells were analyzed using flow cytometry for cell surface markers characteristic of the proinflammatory and anti-inflammatory phenotypes. Additionally, polarized cells were suspended in basal medium for 48 hours. Following the incubation period, the conditioned medium was collected and analyzed using a multiplexing bead assay to detect inflammatory cytokine concentrations.

Additionally, a single randomized percutaneous muscle biopsy was collected from 5 old subjects. Muscle biopsy samples were cut, weighed, digested in enzymes and seeded on tissue culture plates for 6 days, with the medium being changed every 48 hours. After 6 days of incubation, myoblast isolation was performed using a magnetic bead sorting kit for $CD56^+$ cells (21). Cells were grown to confluency (70%), then frozen in liquid nitrogen for later use.

When all samples had been collected, myoblasts were pooled and seeded at a density of 1.2×10^4 and 2.4×10^4 cells per well for proliferation and differentiation experiments, respectively. Proliferation was tested by suspending myoblasts in macrophage-conditioned medium combined with 5-Ethynyl-2'-deoxyuridine (EdU) for 24 hours. Differentiation experiments were performed by suspending myoblasts in macrophage-conditioned medium for 72 hours, after which cells were stained for myosin heavy chain (MyHC) and myogenin expression.

Brief Results

Aim 1a

Macrophages treated with polarizing cytokines displayed a greater proportion of cell surface markers corresponding to the respective treatment. For example, macrophages treated with IL-4 had a greater proportion of CD206. Similarly, IL-10 treatment increased the expression of CD163. As hypothesized, aged macrophages showed an increased sensitivity to IL-10 treatment, as the overall expression of CD163 was greater in old macrophages relative to young.

Aim 1b

Contrary to the hypothesis, aged macrophages did not secrete an increased proportion of anti-inflammatory cytokines relative to the young. In fact, cytokine concentrations were generally higher in the young. Of particular interest were the cytokines IL-6 and TNFa, which have been shown to strongly influence satellite cell behavior. The cytokines IL-6 and TNFa were significantly greater in the young macrophages treated with interferon-gamma, and may help explain why myoblasts from the cell culture experiment were more active when treated with young macrophage-conditioned medium.

Aim 2

As hypothesized, old myoblasts treated with young macrophage-conditioned medium showed an increased capacity to proliferate, and, in some cases, differentiate when compared to the myoblasts treated with old macrophage-conditioned medium. Furthermore, regardless of age, macrophage-conditioned medium was significantly more effective at inducing myoblast proliferation and differentiation than basal medium alone.

MANUSCRIPTS

STUDY I

Acute Extracellular Matrix, Inflammatory and MAPK Response to Lengthening Contractions in Elderly Human Skeletal Muscle

Published: *Exp Gerontol.* 2018 Jun;106:28-38. doi: 10.1016/j.exger.2018.02.013.

Highlights

- Dysregulated inflammatory, extracellular matrix and MAPK cell signaling responses are observed following acute muscle damage in aging animals.
- We tested whether old humans exhibit the same dysregulated response following nonpathological skeletal muscle damage (lengthening muscle contractions).
- Aged skeletal muscle shows greater fatigue resistance during lengthening contractions relative to young muscle.
- In the 3 days following muscle damage, irregularities appear in the inflammatory, extracellular matrix and cell signaling response of older subjects.
- Human aging is accompanied by alterations to important stress response elements known to be essential for effective muscle repair and adaptation.

Abstract

To uncover potential factors that may be involved in the impaired regenerative capacity of aged skeletal muscle, we comprehensively assessed the molecular stress response following muscle damage in old and young individuals. Ten young (22.7 ± 2.25 yrs) and 8 physically active old (70.9 ± 7.5 yrs) subjects completed a bout of 300 lengthening contractions (LC), and muscle biopsies were taken preexercise and at 3-hour, 24-hour, and 72-hour postexercise. Both age groups performed the same amount of work during LC, with the old group displaying a

resistance to LC-induced fatigue during the exercise. Muscle damage was evident by soreness and losses in isokinetic force and power production, though older subjects experienced reduced force and power losses relative to the young group. The acute extracellular matrix (ECM) response was characterized by substantial increases in the glycoproteins tenascin-C and fibronectin in the young, which were blunted in the old muscle following damage. Old muscle displayed a heightened and asynchronous inflammatory response compared to young muscle, with higher expression of MCP-1 that appeared at later time points, and increased NF-κb activity. Expression of the stress-related MAPKs P38 and JNK increased only in the old groups following muscle damage. In summary, aberrations appear in the inflammatory, ECM and MAPK responses of aged skeletal muscle following muscle damaging LC, any of which may individually or collectively contribute to the deterioration of muscle repair mechanisms that accompany aging.

Introduction

Skeletal muscle has a relatively high capacity for repair following both physiologic (ie, exercise) and pathologic (ie, muscle strain) stress. Nevertheless, like many biological tissues, its reparative potential appears to decline with advanced age (22, 23). Loss of precise muscle repair through the decades of adult life likely potentiates the physiologic attrition of muscle and contributes to the eventual deterioration of muscle functional capacity and its associated co-morbidities.

In young organisms, successful muscle repair following stress is dependent on a set of acute, transient changes in the myofiber extracellular environment. The most well-characterized of these transient alterations include: increased inflammatory activity (16, 24, 25), the appearance of a transitional extracellular matrix (26), and activation of muscle stem cells (27).

Moreover, transient changes in the activity of stress-related intracellular signaling pathways, most notably the mitogen-activated protein kinases (MAPK), have been shown to mediate muscle repair mechanisms in animals (28) and humans (23).

In nonpathological muscle damage, inflammation is a tightly regulated process that is generally regarded as essential for effective reparative adaptation (29). For example, genetic knockout of individual cytokines and/or their receptors, or the restriction of immune cell entry into skeletal muscle impedes muscle regeneration in animal models (24, 25). Likewise, though somewhat less studied than inflammation, the transient upregulation of extracellular matrix (ECM) glycoproteins appears to be important in mediating muscle repair. Termed the "transitional matrix" by Calve et al (26), the upregulation of hyaluronic acid, tenascin-C and fibronectin direct cellular regenerative efforts by providing important cues for muscle stem cell activation and migration. We have recently characterized the appearance of the transitional matrix following muscle damage in humans (30). A compelling similarity between inflammation and ECM alteration is their collective dysregulation in aging. For instance, many age-related diseases (eg, type II diabetes, heart failure and rheumatoid arthritis) are associated with an overactive or misguided inflammatory environment. In the same manner, fibrosis of tissue and organ systems (eg, heart, lung) is a hallmark of the aging phenotype (31, 32).

Given the dependent nature of muscle regeneration on these transient events and their corresponding dysregulation in biological aging, we hypothesized that skeletal muscle repair in older individuals would be characterized by a diminished and asynchronous inflammatory, ECM, and cell signaling response relative to muscle repair in younger individuals. In the following report, we used immunohistochemical and high-throughput multiplexing analyses to interrogate the transient muscle response in old and young individuals for 3 days following muscle damage.

Our findings confirm that abnormalities arise in the response of older muscle to damage throughout the first 3 days of muscle repair.

Methods and Materials

Ethical Approval

Subjects were informed of all procedures and potential risks and signed a written, informed consent document approved by the Brigham Young University Institutional Review Board. The study conformed to the standards set by the Declaration of Helsinki, except for registration in a database.

Subjects

Eleven healthy young (aged 22 ± 2 yrs, n = 11) and 8 old (aged 71± 7 yrs, n = 8) men and women volunteered to participate in this study. The young group consisted of 7 men and 4 women. The old group consisted of all men. All subjects underwent a routine health questionnaire and screening. For the young group, subjects' habitual activity ranged from sedentary to mildly active, but none was actively training in any particular sport, nor had they participated in a lower body or upper body strength-training program for at least 6 months before participating in the study. For the old group, subjects were primarily screened on the basis of their ability to complete the exercise protocol. This necessitated that we recruit a relatively fit old population. Though we collected no objective measures of fitness, the majority of old subjects were regular exercisers and participated in both aerobic and resistance training on some days of the week. Old subjects were medication free with the exception of one subject who reported taking Lisinopril for high blood pressure and Pravastatin to lower cholesterol. All subjects agreed to refrain from participating in new physical activity or taking oral or topical analgesics for the duration of the study.

Study Design

The study consisted of 4 laboratory visits. Subjects reported to the laboratory on their first day and were familiarized to the Biodex System 4 dynamometer (Biodex Medical Systems, Shirley, NY). Muscle strength and soreness baseline measures were assessed and a preexercise control biopsy was taken from the vastus lateralis muscle of a randomized leg that would not be exercised in the study. Twenty-four hours after the preexercise biopsy, subjects returned to the lab to perform 300 maximal LC's on the leg opposite the randomized nonexercise leg. This protocol has been used by us and others to induce transient muscle damage (15, 30). Following completion of the muscle-damaging exercise, subjects rested in the lab for 3 hours, after which a biopsy was taken from the vastus lateralis muscle of the exercised leg. The subjects then returned to the laboratory 24 hours and 72 hours postexercise to obtain muscle strength and soreness measurements and to have muscle biopsies taken from the vastus lateralis muscle of the exercised leg (Figure 1.1).

Muscle Biopsy

Percutaneous needle biopsies were taken from the vastus lateralis muscle. The first biopsy was taken from the nonexercised leg before the exercise interventions. Three subsequent biopsies were taken at 3 hours, 24 hours, and 72 hours postexercise. Under local anesthesia (2% lidocaine), a small incision was made into the skin and fascia, and the biopsy needle was inserted into the muscle. With the use of manual suction, 75 to 150 mg tissue was withdrawn. Muscle samples were then separated from any fatty tissue and divided into 25 to 50 mg portions. Portions of tissue designated for protein were frozen immediately in liquid nitrogen. Tissue portions designated for sectioning and microscopic analysis were mounted on a cork with tragacanth gum and frozen in isopentane cooled in liquid nitrogen. Biopsy insertions that were

performed on the same leg were placed 5 cm proximal to the last insertion to minimize potential confounding effects from previous biopsies (33) . However, as samples were only taken from the exercised leg postexercise, we cannot rule out that the observed changes may have been affected by repeated biopsies.

Strength Assessment

Functional muscle capacity was measured on the Biodex dynamometer (Biodex Medical Systems, Shirley, NY). Before the strength trials, subjects were positioned so that their knee joint aligned with the axis of the dynamometer. The lever arm was then attached to each subject's ankle 3 cm above the lateral malleolus. The positioning for each subject remained identical throughout the study. Concentric isokinetic torque and power output were measured at a velocity of $60° \cdot sec^{-1}$. Subjects completed 3 maximal contractions of 3 to 5 seconds each per protocol, respectively, with a 1-minute rest between each test. For every contraction, subjects were instructed to use as much force as possible in their motions. Consistent verbal encouragement was given for each repetition. Peak isokinetic torque values were defined as the highest attainable value from the 3 trials, while power values were the calculated average for the duration of the contraction with an intraindividual coefficient of variation ($\leq 5\%$).

Soreness

Soreness was evaluated using a visual analog scale (VAS). A 100-mm line labeled from 0 mm to 100 mm with 0 mm indicating "no pain" and 100 mm indicating "unbearable pain" was used. Subjects were first instructed to perform two hip/knee flexions and extensions from a seated position. The chair height was adjusted for each subject so that contact with the chair was made at a knee flexion angle of 90°. During the task, subjects were asked to quantify the level of pain experienced in the knee extensor muscles and mark the scale with a single vertical line

accordingly. The distance from the left end of the scale to the mark was taken as the soreness level.

Immunohistochemistry

Eight-micrometer cross sections of muscle biopsy tissue samples were cut using a cryostat at −25°C. Samples were mounted to Superfrost slides and air dried for 10 min. For slides that were stained for type I myosin heavy chain (MyHC), tenascin-C, or fibronectin, sections were fixed in 2% paraformaldehyde (Sigma-Aldrich, St. Louis, MO) for 7 or 10 min. Following fixation, sections were washed in phosphate-buffered saline (PBS) solution 3 times for 3 minutes each time. Sections were then blocked in 0.2% Triton X-100, 2% bovine serum albumin (BSA), 5% fetal bovine serum (FBS) solution for 30 or 60 min at room temperature in a humidified container. Sections were incubated in the appropriate primary antibody in a humidified chamber overnight at 4°C. Following several washes, sections were then incubated in the appropriate secondary antibody for 30 min at 37°C. Sections were then washed multiple times and rinsed in ultrapure water. Stained slides were then dried and mounted using Fluoroshield histology mounting medium (Sigma–Aldrich, St. Louis, MO). For hyaluronic acid staining, sections were fixed as described above (2% paraformaldehyde). The samples were then washed in PBS and blocked in Avidin/Biotin blocking solutions (Vector Laboratories, Burlingame, CA) for 15 minutes each. The sample was then placed in a humidified chamber at 4°C and left to incubate overnight in hyaluronic acid binding protein (Calbiochem, Billerica, MA) diluted 1:100 in 1% BSA. The following day the slides were washed in PBS and incubated in DyLight 488 Streptavidin (1:100; Vector Laboratories, Burlingame, CA). Stained slides were washed in PBS, dried, then mounted using Fluoroshield histology mounting medium (Sigma–Aldrich, St. Louis, MO). The following primary antibodies were used: myosin heavy chain I,

IgG2b (1:100; Developmental Studies Hybridoma Bank, Iowa City, IA; BA-D5), tenascin-C, rabbit polyclonal (1:100; Millipore: AB19013, Temecula, CA), fibronectin (1:50; Santa Cruz Biotechnology, Dallas, TX). Secondary antibodies used were: Rhodamine Red IgG2b (1:100; Jackson ImmunoResearch Laboratories, West Grove, PA), DAPI (1:150; Thermo Scientific, Rockford, IL), Alexa Fluor 488 goat anti-mouse (1:200; Abcam, Cambridge, MA), DyLight 488 Streptavidin (1:100; Vector Laboratories, Burlingame, CA).

Quantification of Immunofluorescent Images

All quantification of immunofluorescent images was carried out by an investigator that was blind to both time point and subject grouping. For MyHC analyses, 1 to 5 (depending on the size of the sample) randomly acquired fields from all subjects at the preexercise time point were imaged. Images were taken using a 20x objective. An average of 41 ± 18 type I and 53 ± 23 type II myofibers from each subject were traced manually and quantified using Olympus cellSens software. Grouping of type I and type II fibers was identified using the "enclosed fiber" method (34), which considers a fiber "enclosed" when it is surrounded by fibers of its own histochemical type (see Figure 1.2 for a representative image of an enclosed type I and type II fiber). In addition, a cross-sectional area of each fiber-type grouping was measured using the same method described above. Quantification of tenascin-C, fibronectin, and hyaluronic acid was carried out by calculating the total immunoreactive area of the entire section (~2–4 10x or 20x images that were taken at the same exposure time). For quantification, the total immunoreactive area was expressed relative to the total area of the imaged section. All analyses were done using Olympus cellSens software.

Protein and Cytokine Magnetic Bead Multiplexing Analysis

Frozen tissue samples were weighed and homogenized with a Total Protein Extraction Kit (Millipore Corporation, Billerica, MA) at a ratio of 9 µl per mg tissue with the addition of a protease and phosphatase inhibitor cocktail (Thermo Scientific, Rockford, IL). Tissue disruption was performed on ice using a glass-on-glass dounce homogenizer. The homogenate was centrifuged at 10,000 g, 4°C for 10 minutes. The supernatant was analyzed in triplicate for total protein concentrations with the BCA Protein Assay Kit (product# 23227, Thermo Scientific Pierce, Rockford, IL). Supernatant was stored at −80°C. The Luminex Magpix multiplexing platform (Luminex xMAP Technology, San Diego, CA, USA) was then used for multianalyte profiling of biopsy sample homogenates. Protein in muscle homogenates were measured using 6-plex TGF-β (Cat# 48-614MAG) and 9-plex multipathway total magnetic bead kits (Cat# 48-681MAG). Cytokines in the muscle homogenate were measured using an 11-plex Human Cytokine/Chemokine magnetic Bead Panel Kit (Cat# HCYTOMAG-60K) in compliance with manufacturer's recommendations. Briefly, antibody-conjugated magnetic beads were incubated with 25 µL of tissue homogenate (15 µg protein/well) overnight at 4°C on a plate shaker. Bead-complexes were then washed and incubated in detection antibodies for 1 hour on a plate shaker at room temperature. This was followed by incubation in streptavidin phycoerythrin for 15 minutes on a plate shaker at room temperature, with an additional 15-minute incubation in amplification buffer. Bead-complexes were resuspended in assay buffer and mixed on a plate shaker for 5 minutes, and then analyzed on a MAGPIX multiplex platform. Mean fluorescent intensity (MFI) values were recorded and used for data analysis. Data were analyzed using Milliplex Analyst 5.1 software (Millipore Corporation, Billerica, MA, USA).

Statistics

Muscle fiber characteristics (CSA, fiber-type, and fiber grouping) were determined at the preexercise time point and a student's t-test was used to test for differences between young males and females as well as between young and old groups. A repeated measures mixed model analysis with main effects for group, sex, and time were used in conjunction with the interaction of group x time to test changes within and between groups for ECM glycoprotein, protein, and cytokine response data, while the covariate of body mass index (BMI) was added to the model for functional testing data. A Tukey-Kramer HSD test was performed post hoc when the fixed effect test revealed a significant *p*-value for main effects or the group x time interaction. To normalize distributions and homogenize variance, the following variables were log transformed; Soreness, IL-8, MIG, IP-10, I-TAC, MCP-1, and tenascin-C. Following statistical analysis, log-transformed data were back-transformed and data presented as the geometric mean with upper and lower 95% confidence intervals (35). Prism Graphpad (V6.0b; San Diego, CA, USA) was used to create figures. JMP® Pro (V12.2; SAS Institute, Cary, NC, USA) was used for all statistical analysis. Results were considered statistically significant at $p < 0.05$.

Results

Subject Characteristics and Exercise Performance

Subject characteristics and exercise performance data for the young and old groups are presented in Table 1.1. Few studies have investigated the effect of damaging exercise on skeletal muscle parameters in women. Thus, we felt it was important to include women in this study. Unfortunately, we were unable to recruit women in the older group that were capable of performing the difficult bout of LC's. Rather than omitting the data from the young women, we have included sex in the statistical model. Where a main effect of sex was detected, a separate

analysis was performed without the women. The removal of the women from the analysis did not change the statistical significance of old and young for any of the measured variables. There were no significant differences between young and old for anthropometric measures. Likewise, the total amount of functional work, average torque and average power output that was completed during the bout of LCs was similar between groups. However, an interesting observation was that the rate of functional decline (fatigue) was greater in the young relative to the old throughout the 30 sets of LCs for average work and power output, as indicated by a significant group x time interaction ($p < 0.05$) (Figure 1.3), but not average torque (group × time: $p = 0.63$).

Muscle Fiber Characteristics

Muscle fiber characteristics for the young and old groups can be found in Table 1.2. Unexpectedly, type I and type II myofiber cross-sectional area was similar between the young and old groups (type I, $p = 0.415$) (type II, $p = 0.474$), even when removing the young females from the analysis (type I, $p = 0.406$) (type II, $p = 0.118$). However, despite similar myofiber CSA, there was a significantly greater proportion of type I fibers in the old relative to the young group ($p = 0.023$). Furthermore, for fiber-type grouping, we did detect a baseline increase in grouped type I fibers in the old, as measured by the ratio of type I grouped CSA per total CSA ($p = 0.018$). Type II fiber type grouping was similar between young and old ($p = 0.522$) (Table 1.2).

Functional Measures

Muscle soreness, peak isokinetic torque and power were analyzed to evaluate functional capacity and used as indirect measures of muscle damage. Following the bout of LC, young and old groups had a similar increase in muscle soreness (time: $p < 0.0001$), peaking at 24 hours and remaining elevated at 72 hours after the bout of LC's for both young and old groups (group: $p =$

0.33) (Figure 1.4A). Baseline peak torque (young: 203.8 ± 50.1 vs old: 155.1 ± 29.7 N • m, $p < 0.01$) and average power (young: 129.1 ± 26.7 vs old: 94.5 ± 21 watts, $p < 0.05$) was significantly higher in the young (Figure 1.4B-C). Following the bout of LC's, the functional response was different between young and old groups, indicated by a significant group × time interaction for isokinetic peak torque ($p = 0.0009$) and average power ($p = 0.0014$). Post hoc testing revealed that peak torque and average power were markedly reduced from baseline values at 0, 24 hours and 72 hours in the young. Conversely, peak torque and average power declined significantly at 0 hours post-LCs in the old, yet returned to baseline levels by 72 hours (Figures 1.4D–E).

Extracellular Matrix Response

ECM remodeling and the appearance of a transitional matrix (ECM) have been observed in models of muscle damage and shown to be necessary for effective regeneration (26). To measure the appearance of the transitional matrix, we assessed the immunoreactivity of ECM glycoproteins tenascin-C and fibronectin in conjunction with the glycosaminoglycan hyaluronic acid. The percentage of total muscle area that was immunoreactive for tenascin-C increased 4.8 times (95% confidence: 2.3 to 10.1) preexercise to 24 hours postexercise in the young ($p < 0.0001$) and remained 3.2 times larger than baseline values at 72 hours following the exercise (95% confidence: 1.5 to 6.9, $p = 0.0003$). Conversely, tenascin-C was unchanged preexercise to 24 hours ($p = 0.67$) and 72 hours ($p = 0.41$) postexercise in the old (group × time: $p = 0.026$) (Figure 1.5A). Fibronectin immunoreactivity was increased significantly from preexercise to 72 hours postexercise among young (5.6 ± 4.4 to 12.8 ± 5.9%) and old (10.5 ± 4.6 to 13.6 ± 3.4, time: $p < 0.0001$) subjects. However, a significant main effect for group shows that overall fibronectin immunoreactivity was greater in the old (group: $p = 0.04$) (Figure 1.5B). No group

differences were observed for hyaluronic acid expression following the bout of LCs, yet given the large variability between subjects and time points, trending differences may represent potential increases over time (time: $p = 0.08$) (Figure 1.5C).

TGF-β Signaling

The transforming growth factor beta (TGF-β) signaling pathway regulates the synthesis of many ECM-related structural and nonstructural components and was measured to assess ECM-remodeling activity at the cell signaling level. The most marked change in TGF-β signaling was noted in the expression of TGF-βRII (Figure 1.6A). Expression of the receptor had an overall increase of 1.5 ± 0.82 fold, increasing from 92.9 ± 30.3 to 141.2 ± 25.8 MFI preexercise, to 72 hours postexercise (time: $p < 0.0001$). Additionally, there was a greater overall effect for the old (group: $p = 0.0002$) and female populations (sex: $p = 0.0004$). The expression of phosphorylated Smad3$^{Ser423/Ser425}$ also showed an overall increase of 1.45 ± 0.48 fold, increasing from 39 ± 9.5 to 56.6 ± 11.9 MFI preexercise to 72 hours postexercise for both groups (time: $p < 0.001$) (Figure 1.6C). In contrast, phosphorylated Smad2$^{Ser465/Ser467}$ and total Smad4 protein expression remained unchanged following the bout of LCs (Figures 1.6B, D).

Cytokine and Inflammation-Related Signaling

To determine the extent of inflammation and identify important cytokines that may characterize the aged muscle response to damage, we measured 10 cytokines and assessed the total protein content of the signaling transducer and affecter of transcription (STAT3, STAT5A/B) and nuclear factor kappa-light-chain-enhancer of activated B cell (NF-κB) proteins via multiplexed magnetic bead analyses. As aged skeletal muscle has been characterized to have an elevated presence of inflammatory markers (36), we were surprised that baseline differences were not detected for any of the measured cytokines or inflammatory-related signaling proteins.

Nonetheless, differences were detected following the bout of LCs. Among the cytokines measured, monocyte chemoattractant protein-1 (MCP-1 also known as CCL2), and interleukin-1b (IL-1b) had a significant main effect for group. MCP-1 increased significantly from the preexercise value in both young and old groups (time: $p < 0.0001$), peaking to 6.7 fold at 3 hours postexercise in the young (95% confidence interval: 2.3 to 19.4 fold) and 7.2 fold at 24 hours postexercise in the old (95% confidence interval: 2.2 to 23.6), with the overall response being 2.1 fold greater in the old (95% confidence interval: 1.2 to 4.1, group: $p = 0.019$). Conversely, the overall levels of IL-1b remained lower in the old relative to the young (group: $p = 0.0086$), with a trending effect for time (time: $p = 0.055$). Additionally, monokine induced by gamma interferon (MIG also known as CXCL9), interferon gamma-inducible protein 10 (IP-10 also known as CXCL10), interferon-inducible T-cell alpha chemoattractant (I-TAC also known as CXCL11), interleukin-7 (IL-7) and interleukin-8 (IL-8) all showed a significant effect among biopsy time points for both young and old groups ($p < 0.05$). The remaining cytokines—granulocyte colony-stimulating factor (GCSF), interleukin-6 (IL-6), and interleukin-13 (IL-13)—remained unchanged and can be found in Table 1.3. Interleukin-4 (IL-4), interferon gamma (IFNγ) and tumor necrosis factor-alpha (TNF-α) were undetected in the assay. NF-κB signaling showed a significant main effect for time in both groups (time: $p = 0.001$), peaking at 3 hours postexercise at 1.6 ± 0.56 fold higher than the preexercise value, and remaining significantly elevated out to 72 hours postexercise (Figure 1.7A). NF-κB also showed a near group × time interaction (group × time: $p = 0.055$), while STAT3 and STAT5 protein concentrations were unchanged (Figure 1.7 B-C).

MAPK Signaling

To evaluate the extent of exercise-induced cellular stress, we measured the response of several mitogen-activated protein kinase (MAPK) family members using a multiplexed magnetic bead assay. In the old, a rapid and robust increase was measured for total p38 and JNK proteins following the exercise, whereas no significant differences were detected in the young. Specifically, post hoc analysis revealed that p38 increased 1.70 ± 0.47 fold in the old at the 3-hour postexercise, before returning to preexercise levels (group × time: $p = 0.0043$) (Figure 1.8A). At 3 hours postexercise total JNK protein levels peaked to 2.4 ± 1.3 fold of the preexercise value and remained significantly elevated at 2.07 ± 0.92 fold 24 hours postexercise (group × time: $p = 0.038$) before returning to preexercise levels (Figure 1.8B). A delayed response was measured for phosphorylated ERK1/2$^{\mathbf{Thr185/Tyr187}}$ in both groups, rising significantly from 123.9 ± 137.3 to 203.2 ± 94.1 MFI 24 hours to 72 hours postexercise (time: $p = 0.024$) (Figure 1.8C). The expression of ERK1/2 total protein remained unchanged following the exercise for both groups (Figure 1.8D).

Discussion

The primary objective of this study was to characterize the transient molecular reparative response to muscle damage in aged humans. As prior animal studies have reported irregularities in the acute inflammatory, ECM, and MAPK responses of aged muscle following damage (28, 37), the focus of this study was directed at measuring acute (up to 72 hours) changes in these variables. This is the first study to comprehensively investigate the skeletal muscle cellular and molecular response to a protocol designed specifically to induce nonpathological muscle damage in aged humans. Our data provide the first evidence of significant aberrations in the acute response to damage in otherwise healthy skeletal muscle of aged (> 65 years) adults.

Firstly, we recognize that interpretation of our data must be made within the context of the physical fitness of our elderly subjects, as age-related differences in muscle functional and molecular characteristics have been clearly shown to be dependent on fitness (38). Completion of the stressful LC protocol necessitated that our older subjects be relatively fit. Though we regrettably have no quantitative measures of physical activity, all of our older subjects reported participation in daily bouts of structured physical activity. In fact, the fitness of our older-subject population is perhaps most clearly evident in the observation that myofiber size in the old group was not significantly different than the young group, even when sex was taken into account (ie, women in the young group removed from the analysis). Nevertheless, muscle in the older group did present with other characteristic features of "older" muscle. For example, the older group demonstrated a shift towards a type I myofiber phenotype (39), fiber-type grouping characteristics (40), and displayed lower baseline functional measures. In the sense that our elderly subjects likely represented a uniquely "high-fit" demographic, we find it especially interesting that differences arose between our older and younger subjects following LC. This finding suggests that, regardless of fitness, the aging muscle phenotype is inherently characterized by aberrations in the molecular response to muscle stress.

We used loss of knee extensor force production as our primary measure for muscle damage, as it has been shown to be the most reliable of the indirect damage markers (41). Interestingly, older muscle was less susceptible to LC-induced damage, evidenced by reduced functional losses (torque, power, impulse) and faster recovery following the exercise. This finding is supported by some (42), but not all (43) previous studies, and is also likely influenced by the training status of our old-subject population. While, as expected, older subjects presented with reduced isometric torque and power at baseline compared to the young, an interesting

finding that emerged from the exercise data was the preservation of baseline eccentric force production. Moreover, the older group demonstrated significantly greater fatigue resistance through the exercise session than did the young subjects. These data would suggest that deterioration of eccentric force production with age is less than that of isometric or isokinetic force loss, and that age-related fatigue resistance, previously reported to occur with isometric contractions (44), extends to LC's. The preservation of eccentric force production with aging is supported by previous studies (45, 46). However, this is the first study, to our knowledge, to demonstrate an age-related fatigue resistance to LC.

One of the more compelling insights gained from the present study was that, notwithstanding the relatively youthful appearance of the muscle in the aged group, significant asynchronies appeared in the acute response to muscle damage. Our laboratory and others have recently shown a biphasic ECM-remodeling response in humans, characterized by the transient up-regulation of ECM glycoproteins (termed the "transitional matrix"), followed sequentially by upregulation of structural collagens (30, 47). Studies have demonstrated that appearance of the transitional matrix (tenascin-C, fibronectin, hyaluronic acid) is essential for successful muscle regeneration by providing important cues that drive muscle stem cell regenerative potential (26, 48). Immunohistochemical analyses revealed that, generally, the appearance of transitional matrix components is acutely blunted in old relative to young muscle. Further, aging appears to potentiate the premature activation of TGF-β signaling, a primary pathway mediating collagen expression. It has been long recognized in animal models that restoration of aged muscle following damage is characterized by a shift away from normal regenerative mechanisms towards a state of increased ECM deposition and reduced stem cell activity (49). Our

observations support the idea that dysregulated ECM cues may contribute to age-related ECM accumulation and stem cell dysfunction in humans.

Another hallmark of biological aging is increased systemic inflammation, which can also be present at the level of individual tissues. There is some evidence that aging is associated with increased basal levels of skeletal muscle inflammation (50), yet there is disagreement within the literature (36). Furthermore, much of the human data is limited to mRNA expression of a limited number of cytokines. Even less well-known is how local inflammatory responses differ in old vs. young human muscle following damage. As optimal muscle repair is dependent on sequential inflammatory events, we suspect that the delayed reparative response of aged human muscle (22, 23) may in part be due to dysregulated inflammatory events. Using a high throughput approach, we have significantly augmented the currently available information regarding cytokine protein expression following damaging exercise in humans. There is surprisingly limited data on cytokine protein concentrations in human skeletal muscle following mechanical load. Cytokines have almost exclusively been measured at the mRNA level or using nonquantitative methods (ie, immunohistochemistry). The lack of protein data in the published literature makes comparison of cytokine concentrations obtained via our immunomagnetic bead method difficult, perhaps calling into question the validity of the assay. Nevertheless, cyotkines that responded to LC's in the present study (MCP-1, IL-8) have generally been shown to increase at the mRNA level or at the protein level in nonquantitative assays following eccentric exercise or resistance training (51). Contrary to what we expected, we did not detect any differences in intramuscular inflammation at baseline between our old fit and young subjects. However, the acute response to damage was marked by some differential inflammatory changes between young and old. Collectively, our data suggest that older muscle is characterized by a heightened inflammatory response following

damage, evidenced by higher expression of MCP-1, a trend towards higher IL-8, and increased total NFκB (p65) protein content. Of particular note, the timing of MCP-1 expression varied between groups, peaking at 3 hours in the young, while a greater peak in the old was observed at 24 hours following LC. MCP-1 is an important macrophage attractant, and its expression is capable of mediating macrophage polarization towards an M2 phenotype (52). Macrophages, particularly those of an M2a phenotype, are present at high levels in pathologic muscle (ie, Duchenne muscular dystrophy), and are primarily responsible for the shift towards a profibrotic state (53). Based on the present data, we speculate that the heightened and persistent inflammatory state may be, in part, responsible for the diminished reparative capacity of aged muscle.

As a master regulator of gene transcription, the MAPK signaling pathway has been shown to couple cellular stress to adaptive responses in skeletal muscle, the dysregulation of which can impede skeletal muscle adaptive potential (54). However, human studies that have investigated the temporal response of MAPK signaling to acute muscle damage are limited, especially in models of aging. Interestingly, our data both contradict and support previous findings from human and animal studies, respectively. While we measured a significant increase in total p38 and JNK protein levels 3 hours following the bout of exercise, Williamson et al showed no change in total MAPK (ERK, p38, and JNK) levels of young and old adult skeletal muscle immediately following an acute exercise bout. In fact, p38 and JNK phosphorylation increased in the young and declined in the old, indicative of metabolic adaptation (55). Conversely, animal studies support our findings that aged skeletal muscle irregularly upregulates p38 MAPK signaling and results in premature differentiation of satellite cells, loss of their self-renewing capacity and dysfunctional myogenic activity (28). There is accumulating evidence to

suggest that the mode, timing, and cell population involved in the activation of MAPK signaling is of great importance to the adaptive response of the muscle. For example, intense exercise stimulates the immediate activation of the MAPK family of proteins to regulate adaptations in glucose uptake (56) and mitochondrial function (57). On the other hand, ligand activation of the MAPK pathway is associated with inflammation (58), cellular growth and differentiation (59). Thus, while our data appear to illustrate a timing discrepancy that would imply a potentially dysfunctional myogenic response in the old group (28), we cannot confidently make that conclusion with the current data. However, this is the first study to investigate MAPK signaling in human muscle following a damaging stimulus of this magnitude, and the data support the findings of the recent animal literature, and indicate a need for more detailed studies to identify specific roles for MAPK signaling in the reparative response of aged muscle.

In conclusion, we have shown that skeletal muscle of relatively healthy, physically active older individuals is characterized by aberrations in the acute response to physiological stress. The deviant response is manifest in 3 key facets of the reparative process, namely, early ECM remodeling, inflammation, and MAPK signaling. Though the findings presented in this study are primarily observational in nature, we speculate that the dysregulation and/or asynchronies noted within these responses may potentiate the loss of myogenic potential and increased fibrosis that accompanies human muscle aging.

Figure 1.1: Exercise Study Design. Young and old subjects performed an exercise bout of 300 eccentric (lengthening) contractions on a Biodex dynamometer. Indirect measures of muscle damage (soreness and strength) were tested prior to and immediately, 24 hours, and 72 hours after the exercise bout. A single muscle biopsy was collected from the nonexercised leg prior to performing the exercise and 3 biopsies from the exercised leg after 3 hours, 24 hours, and 72 hours postexercise.

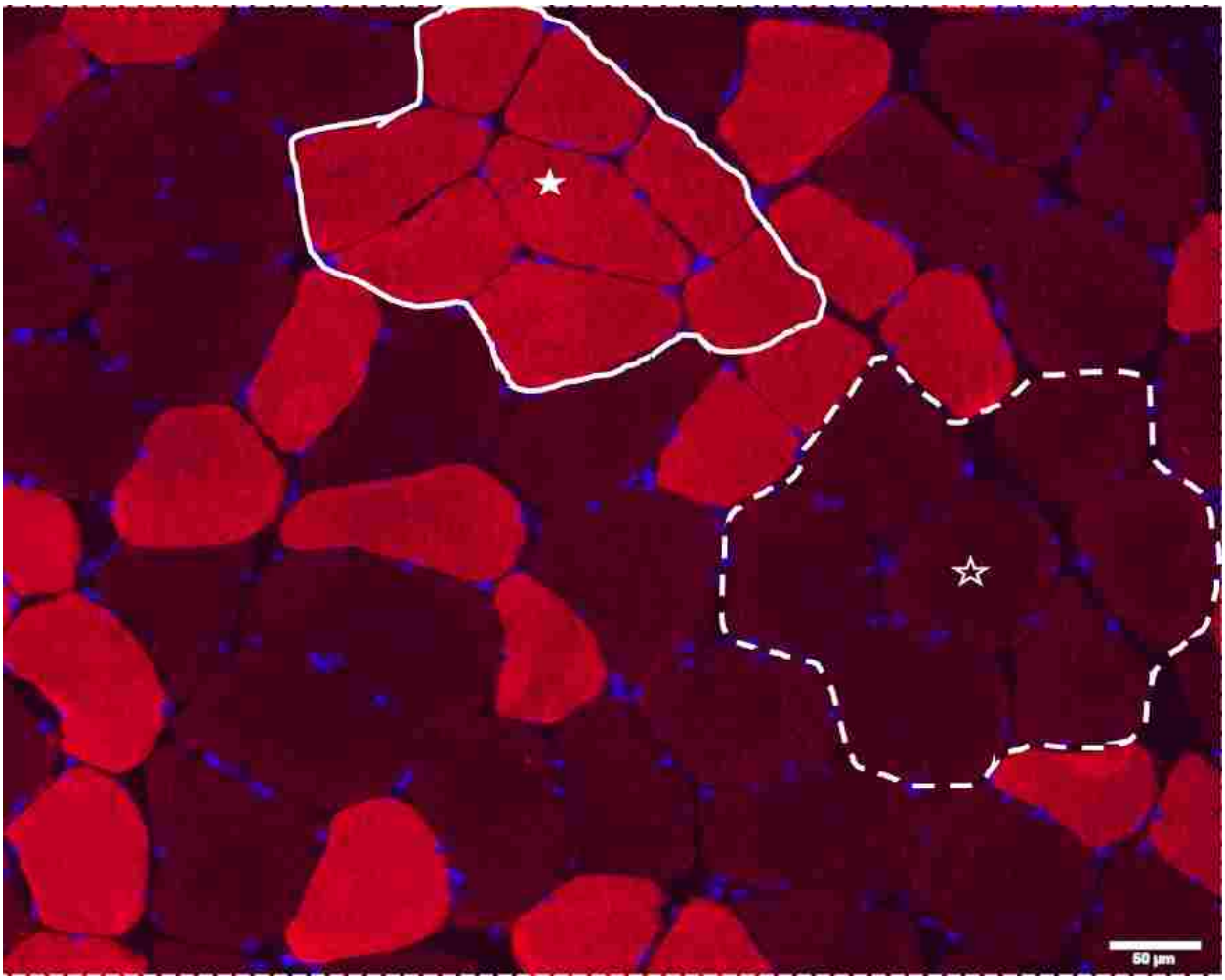

Figure 1.2: Muscle Fiber Analysis. Representative fluorescent image of a double-stained 8 µm section from an Old subject for nuclei (DAPI) and type I myosin heavy chain. Stars identify "enclosed fibers" with a solid line showing representative type I and dotted line type II fiber grouping. Scale bar = 50 µm.

Table 1.1. Subject Characteristics and Exercise Performance

Group	Age (years)	Sex	Height (cm)	Weight (kg)	BMI, kg/m^2	Total Work (kJ)	Total Torque Output (N•m)	Total Power Output (watts)
Young (n = 11)	22.2 ± 2.2	Males (7) Females (4)	174.3 ± 7.5	76.3 ± 14.7	25.1 ± 4.7	44.2 ± 13.1	50148 ± 13011	28105 ± 6985
Old (n = 8)	70.9 ± 7.3	Males (8)	175.3 ± 6.8	88.1 ± 15.1	28.6 ± 4.3	47.9 ± 10.6	54450 ± 11507	30825 ± 5405

Notes: Data are means ± S.D.; BMI, body mass index.

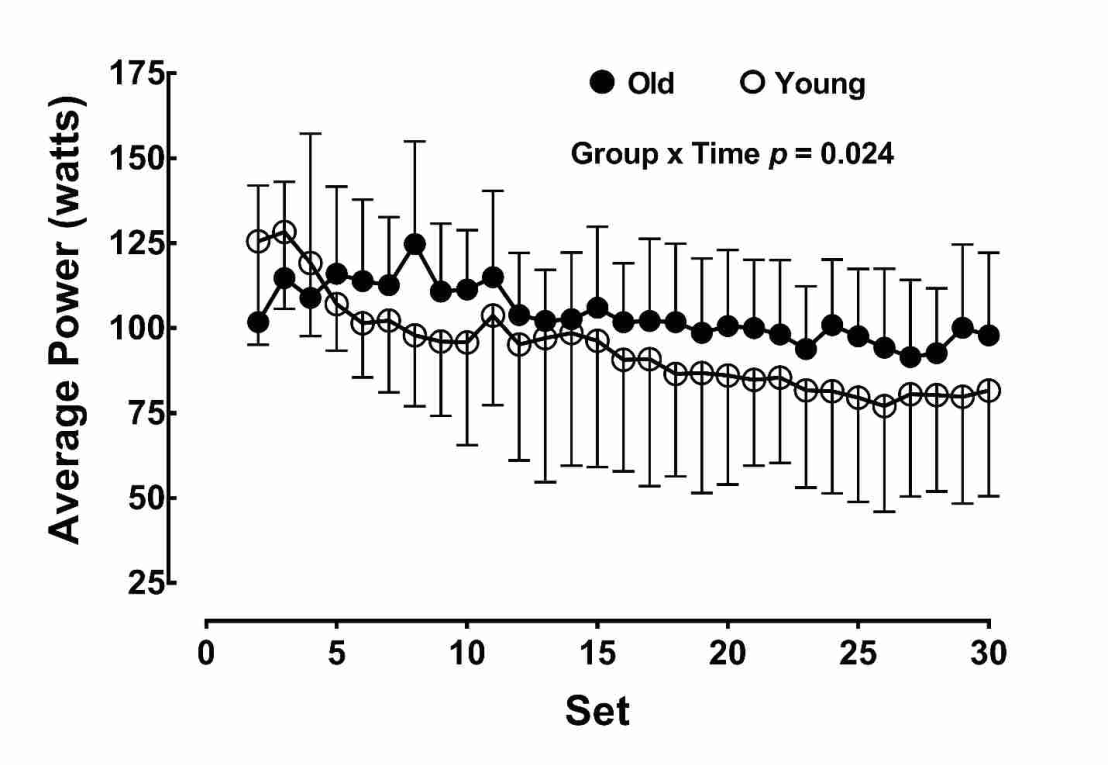

Figure 1.3: Exercise Performance. Exercise fatigue was assessed using the average knee extensor power output per set (10 repetitions) through the duration of the exercise protocol (30 sets). Data are means ± SD

Table 1.2. Baseline Muscle Fiber Characteristics

	Fiber CSA (μm^2)	Fiber %	Fiber Grouping % CSA
Young			
Type I	5469 ± 1225	37.7 ± 13.8	0.9 ± 1.2
Males	5379 ± 1036	35.8 ± 11.9	1.2 ± 1.5
Females	5370 ± 1419	30.5 ± 8.3	0.3 ± 0.7
Type II	5865 ± 1596	62.3 ± 13.8	17.4 ± 15.1
Males	6533 ± 1282	64.2 ± 11.9	17.4 ± 18.5
Females	4506 ± 1469#	69.5 ± 8.3	17.5 ± 10.8
Old			
Type I	5344 ± 1341	45.2 ± 10.8*	6.3 ± 6.2*
Type II	5823 ± 927	54.8 ± 10.4*	13.3 ± 10.4

Notes: Data are means ± SD; CSA, cross-sectional area; fiber %, number of fiber-type-specific fibers as a percentage of the total number of fibers; fiber grouping % CSA, fiber-specific grouping CSA as a percentage of the total CSA. *Significant difference between groups; #Significant difference between young males and females ($p < 0.05$).

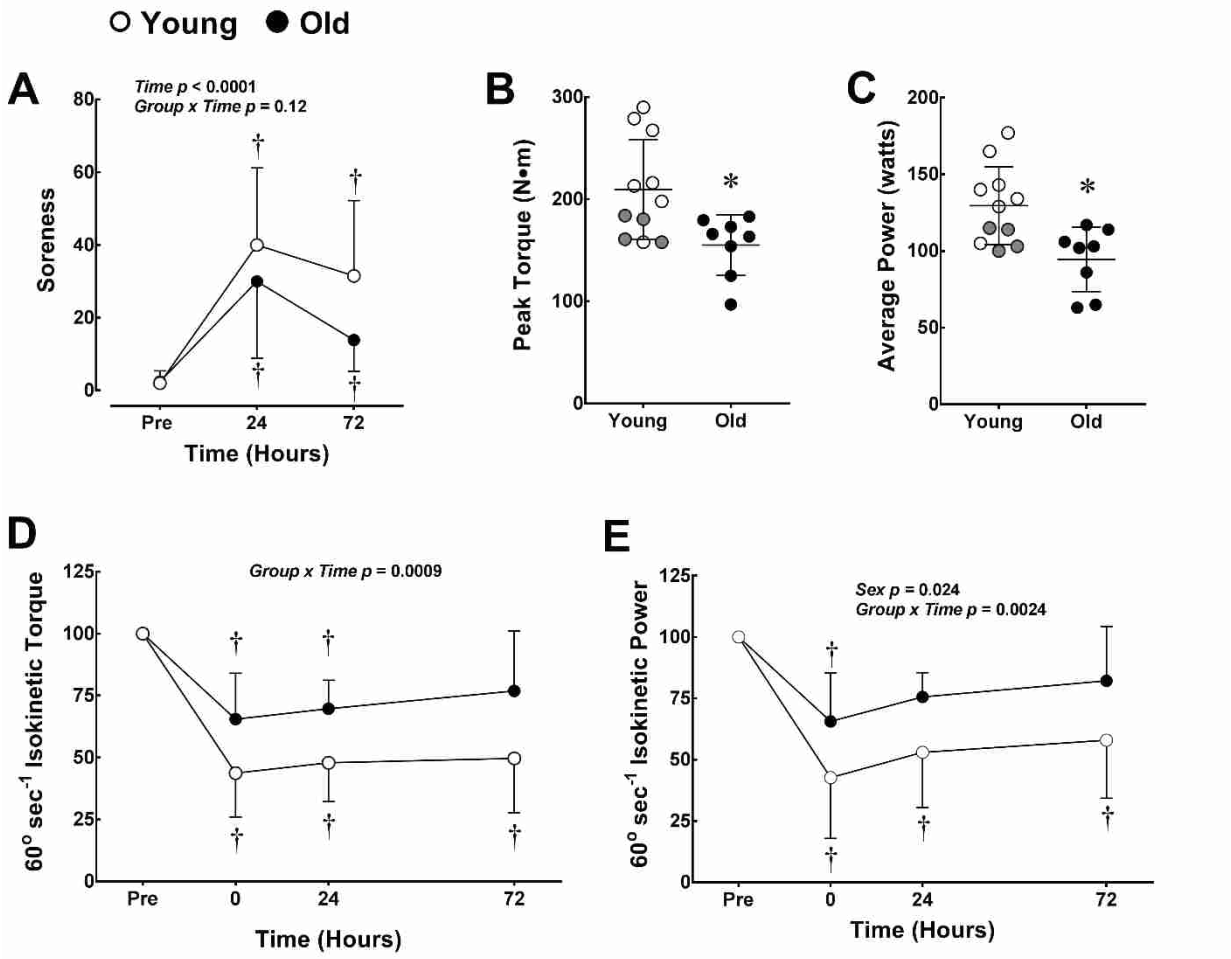

Figure 1.4: Functional Data. Delayed onset muscle soreness and functional characteristics were used as indirect measures of muscle damage following the bout of lengthening contractions (LC). (A) Soreness was measured using a visual analog scale (VAS) prior to, and at 24 hours and 72 hours following the bout of LC. Soreness data were log-transformed for statistical analysis and presented as back-transformed data of the geometric means with upper and lower 95% confidence intervals. Baseline values for peak torque (B) and average power (C) output were measured prior to the bout of LCs. Peak torque (D) and average power (E) output were normalized to show the percent of functional decline at 0, 24 hours and 72 hours. †Significantly different from the preexercise value ($p < 0.05$). Grey circles in (B–C) represent individual data points for females in the young group. Peak torque, average power and 60° isokinetic torque and power data are means ± SD

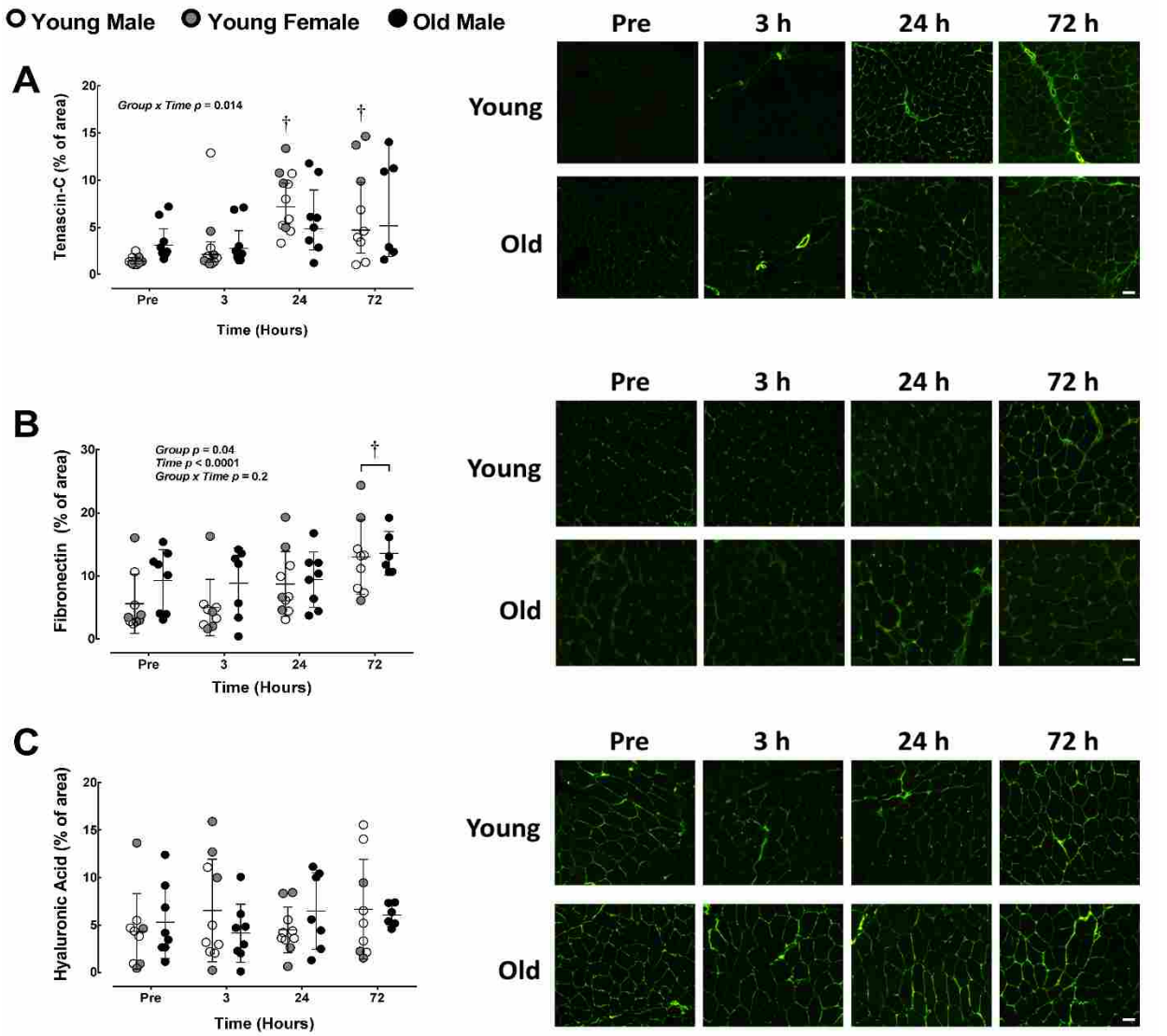

Figure 1.5: Transitional Matrix. The expression of extracellular matrix-related proteins **(A)** tenascin-C, **(B)** fibronectin and **(C)** hyaluronic acid were measured as a percentage of the total image area and are shown with representative 10x and 20x images for the preexercise and 3-hour, 24-hour, and 72-hour time points following the bout of LCs. Tenascin-C data are geometric means ± upper and lower 95% confidence intervals. Fibronectin and hyaluronic acid data are means ± SD; Tenascin-C Scale bar = 100 μm; Fibronectin and Hyaluronic Acid scale bars = 50 μm; †Significantly different from the preexercise value ($p < 0.05$).

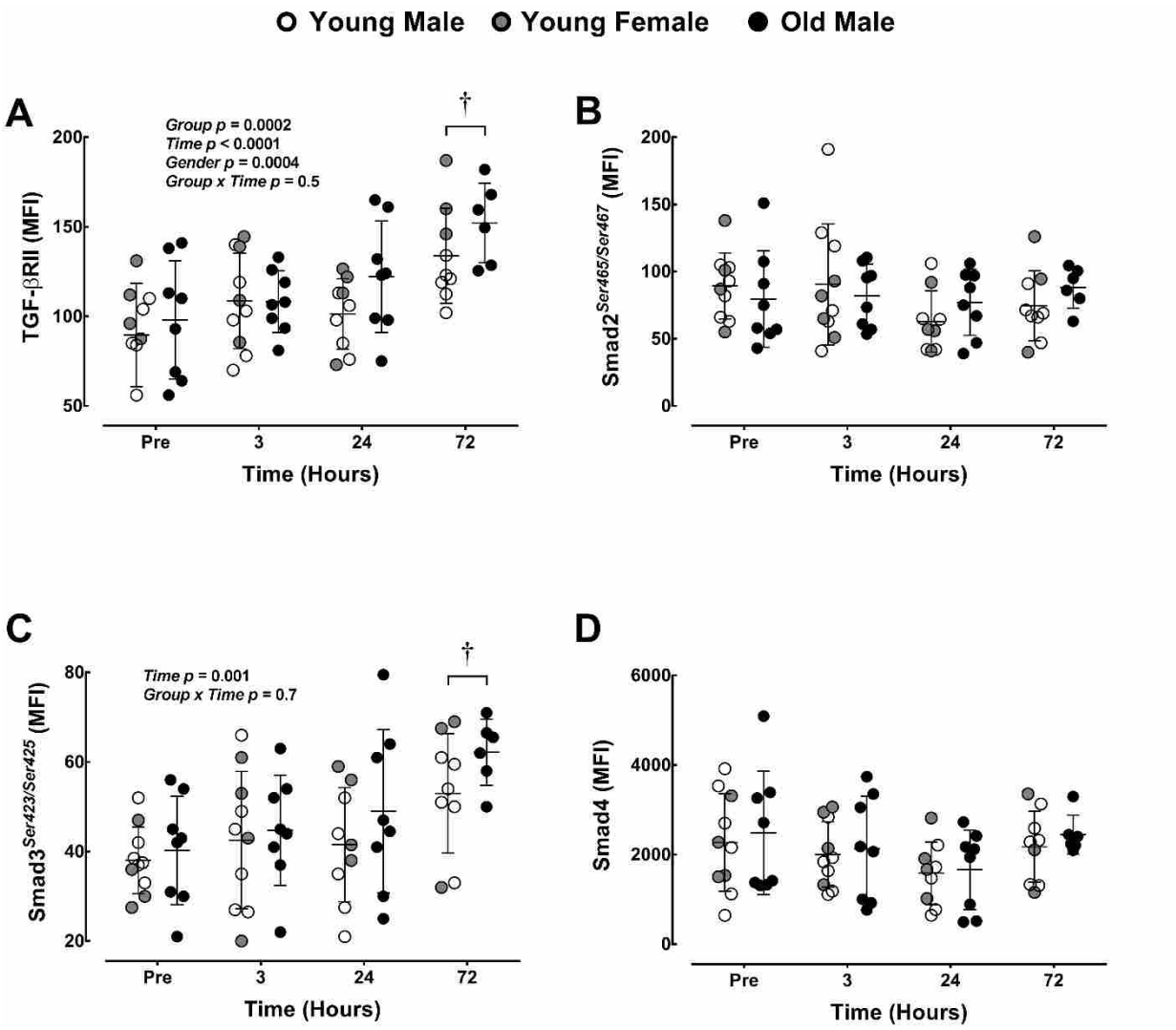

Figure 1.6: TGF-β. TGF-β signaling in skeletal muscle following a bout of LCs, assessed by a multiplexed magnetic bead assay. Shown are the median fluorescent intensity (MFI) values for (A) total TGF-β receptor type 2 (TGF-βRII) protein, (B) phosphorylated Smad2 at Ser465/Ser467, (C) phosphorylated Smad3 at Ser423/Ser425 and (D) total Smad4. Data are means ± SD; †Significantly different from the preexercise value ($p < 0.05$).

Table 1.3. Cytokine Concentrations. *Cytokine concentrations from skeletal muscle biopsy samples preexercise and 3 hours, 24 hours, and 72 hours following a bout of exercise consisting of 300 maximal lengthening contractions.*

Cytokine	Abbreviation	Group	Preexercise (pg ml^{-1})	3 h Post (pg ml^{-1})	24 h Post (pg ml^{-1})	72 h Post (pg ml^{-1})	Sex	Group	Time	Group × Time
Monokine induced by gamma interferon	MIG	Young Old	198.2 ± 102 137.3 ± 32	170.8 ± 73.3 148.7 ± 105.2	263.4 ± 126† 311.8 ± 155†	349.8 ± 262.1 191.6 ± 112.4	0.9	0.12	0.0034	0.35
Interferon gamma-inducible protein 10	IP-10	Young Old	12.5 ± 5.3 12.2 ± 4.4	13.7 ± 6.1 21 ± 10.3	108.9 ± 79.3† 207.2 ± 185†	120.6 ± 249† 40.6 ± 31.3†	0.2	0.24	0.0001	0.7
Interferon-inducible T-cell alpha chemoattractant	I-TAC	Young Old	23.6 ± 33.1 19.6 ± 11.8	13.5 ± 3.8 15.4 ± 14.2	57.5 ± 46.2† 82.8 ± 50.3†	22.9 ± 16.1 30.5 ± 17.3	0.1	0.11	0.0001	0.63
Monocyte chemoattractant protein 1	MCP-1	Young Old*	12 ± 4.7 16.6 ± 5.6	108.7 ± 76.6† 87.2 ± 51.7†	64.4 ± 44.9† 214.3 ± 250†	58.1 ± 45.8† 102.8 ± 121†	0.019	0.020	0.0001	0.37
Interleukin 1b	IL-1b	Young Old*	5.5 ± 1.7 4.3 ± 1.4	6.8 ± 2 4.8 ± 1.7	6.6 ± 1.5 3.9 ± 1.3	5.3 ± 2.5 3.2 ± 1	0.9	0.009	0.07	0.5
Interleukin 6	IL-6	Young Old	15.6 ± 5.7 12.9 ± 5.2	12.8 ± 4.4 11.2 ± 4.9	15.4 ± 5.5 16.9 ± 7.7	12.7 ± 5.5 17.2 ± 7.7	0.042	0.24	0.18	0.22
Interleukin 7	IL-7	Young Old	1.8 ± 0.9 1.5 ± 0.6	3 ± 1.6* 1.9 ± 0.9*	2.3 ± 0.8 1.3 ± 0.7	2.1 ± 1.2 1.6 ± 1.2	0.8	0.13	0.045	0.48
Interleukin 8	IL-8	Young Old	1 ± 0.7 2.5 ± 4.1	1.4 ± 1.4 1 ± 0.6	4.8 ± 4.1† 31 ± 48.5†	11.9 ± 17.1† 16.6 ± 18.4†	0.07	0.057	0.0001	0.62
Interleukin 13	IL-13	Young Old	9.9 ± 5.4 12 ± 3.2	11.4 ± 8.1 10.2 ± 4.1	7.3 ± 4.1 11.9 ± 5.7	8.1 ± 5.8 11 ± 6.6	0.7	0.3	0.7	0.4
Granulocyte colony-stimulating factor	GCSF	Young Old	55.9 ± 20.2 48.5 ± 18.7	45.9 ± 22.9 50.9 ± 26	47.6 ± 29.2 42.2 ± 21.9	38.8 ± 33.1 39.2 ± 21.1	0.6	0.9	0.4	0.7

Notes: Data are means ± SD of 10 detectable cytokines. Cytokines were deemed undetectable when the majority (> 50%) of the observations were below the minimum detection limit. The minimum detection limit ranged from 0.4 to 8.6 pg/mL. The 3 undetectable cytokines were: IL-4, interleukin 4; IFNγ, interferon gamma; TNFα, tumor necrosis factor alpha. †Significant time effect ($p < 0.05$); *Significant group effect ($p < 0.05$).

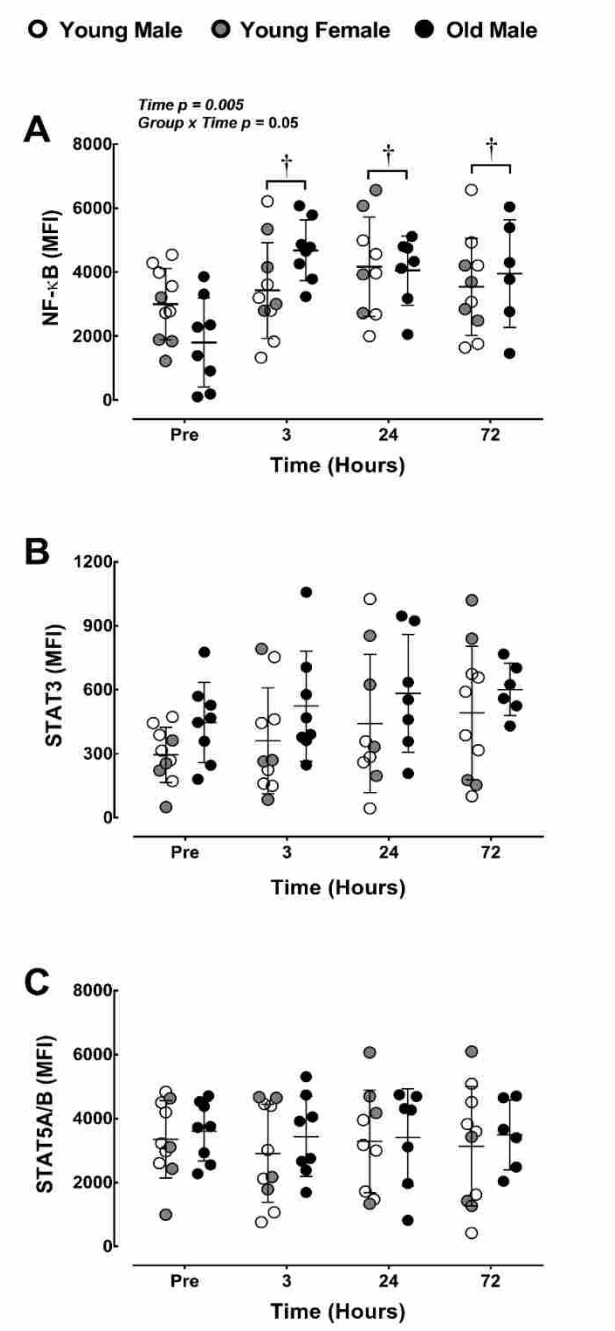

Figure 1.7: Inflammation. Inflammation-related cell signaling of **(A)** NF-κB, **(B)** STAT3 and **(C)** STAT5 were assessed at the protein level using a multiplexed magnetic bead assay and are presented as median fluorescent intensity (MFI) values. **(D)** Illustrative schematic of the inflammatory response in young and old skeletal muscle following acute damage, based on cytokine and cell signaling data. Abbreviations: NF-κB, nuclear factor kappa-light-chain-enhancer of activated B cells; STAT3, signaling transducer and activator of transcription 3; STAT5, signaling transducer and activator of transcription 5. Data are means ± SD; †Significantly different from the preexercise value ($p < 0.05$).

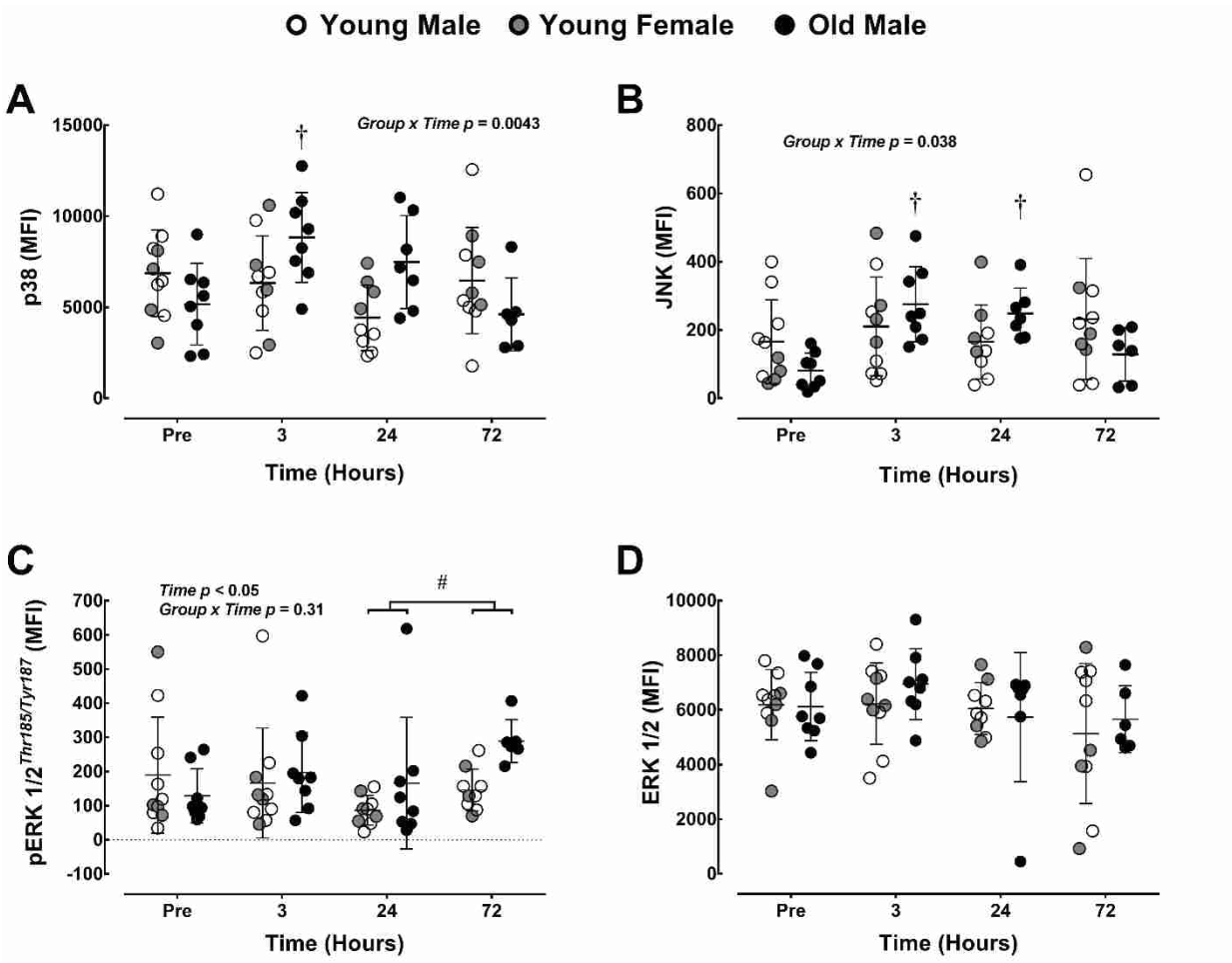

Figure 1.8: MAPK. MAPK signaling pathway in the skeletal muscle of young and old subjects prior to and following a bout of LCs. Shown are the median fluorescent intensity (MFI) values for **(A)** total p38 mitogen-activated protein kinase, **(B)** total c-Jun N-terminal kinase (JNK), **(C)** phosphorylated and **(D)** total extracellular signal-regulated kinase (ERK1/2). Data are means ± SD; #Significantly different between postexercise time points ($p < 0.05$); †Significantly different from the preexercise value ($p < 0.05$).

STUDY II

Macrophage Response to Muscle Damage in Aged Skeletal Muscle: Implications for Skeletal Muscle Repair

Abstract

Aging is associated with a diminished capacity for skeletal muscle repair and adaptation following injury. The immune system, which also declines with advancing age, can have important roles in modulating muscle growth and regeneration, suggesting that aged immune cells, especially macrophages, may contribute to the gradual deterioration of skeletal muscles regenerative capacity. Therefore, the aim of this study was to examine macrophage activity in young and old humans using a nonpathological-muscle damage model. Then, using cell culture experiments, determine the impact of young and old macrophages on primary myoblast activity. We hypothesized that skeletal muscle of older individuals would be characterized by an abnormal inflammatory response following injury, in particular, that macrophages would present with a greater anti-inflammatory phenotype. We also hypothesized that immune cells from young donors would have a greater impact on myoblast behavior relative to older individuals. To test these hypotheses, muscle biopsies were collected prior to and at 3 hours, 24 hours, and 72 hours following a bout of muscle-damaging exercise to examine the acute infiltration and activation of macrophage cells in young and old skeletal muscle tissue. Then, to identify a potential mechanism by which an older immune system may impact muscle repair, cell culture experiments were performed to test young and old macrophage activation, cytokine secretions and influence on human primary myoblasts. We found that macrophage infiltration was similar between groups, yet appearance of proinflammatory macrophages was 25% lower in the old group 24 hours after the exercise. This was coupled with a greater overall proportion of anti-

inflammatory, M2 macrophage accumulation during the early phase of muscle repair. As a follow-up to this finding, we further demonstrate in vitro, that aged macrophages have an increased sensitivity to IL-10 stimulation, which may account for the increased anti-inflammatory macrophage accumulation in vivo. Furthermore, cell culture experiments also showed that macrophages from young individuals secreted significantly more cytokines than macrophages of older individuals, which may help explain why proliferation was 30% higher in myoblasts treated with young macrophage-conditioned medium, and, in some cases, also improved differentiation of human primary myoblasts.

Introduction

Skeletal muscle is a highly plastic tissue with a high capacity to regenerate and adapt following stress. The rather exceptional ability of skeletal muscle to repair and adapt is attributed to a population of myogenic stem cells (satellite cells) that reside just outside the muscle fiber membrane. The unique sublaminar location of satellite cells allows constant monitoring of muscle fiber health, while also facilitating interactions within the extracellular environment. Indeed, the loss of muscle mass and function with advancing age is widely thought to arise from a diminished and unresponsive satellite cell population (60). However, there is evidence that aged satellite cells are capable of healthy regenerative potential if provided with the correct environmental cues. For example, transplantation of skeletal muscle fibers from aged rodents to muscle of young rodents, with satellite cells intact, restores youthfullike regenerative capacity to the aged satellite cells (61), suggesting that factors in the satellite cell niche contribute to their age-related dysfunction. In similar fashion, whole muscle transplantation, as well as blood exchange via heterochronic parabiosis, between young and old rodents also restores aged satellite cell competence (18, 62, 63), suggesting that factors within the systemic circulation are

also partly responsible for the age-related decline of satellite cell function. Therefore, as inflammatory cells have been shown to regulate satellite cell activity (9), and are found in both the systemic circulation and within the extracellular niche (64), they present as viable candidates for altering satellite cell function in the old, and may also serve as a potential therapeutic target for restoring youthful regenerative potential to the elderly.

In young healthy organisms, acute muscle injury is followed by a rapid and robust inflammatory response (10). One of the first and most abundant inflammatory cells to migrate to the damaged tissue is a population of proinflammatory (M1) macrophages. Initially, M1 macrophages prepare the local microenvironment for the rebuilding of new tissue by phagocytosing necrotic muscle fibers, eliminating cellular debris (65), and secreting soluble factors that alter the composition of the extracellular matrix (66). Additionally, M1 macrophages secrete signaling molecules that advance satellite cell proliferation and migration potential (11). Notably, persistence or inhibition of M1 macrophage activity exacerbates tissue damage and delays muscle repair (10, 67, 68). Therefore, a precise and timely transition to an anti-inflammatory, proregenerative (M2) macrophage state is critical to support tissue growth and a return to homeostasis (65, 69). The proregenerative M2 macrophages secrete factors that direct satellite cell differentiation and the rebuilding, remodeling, and maturation of the extracellular matrix (65). Notwithstanding, just as persistent M1 activity can be detrimental to muscle health, so, too, can an overabundance or premature transition to an anti-inflammatory phenotype (58). For example, early secretion of M2-associated cytokines in damaged tissue results in delayed muscle repair, coupled with excessive fatty and fibrotic tissue deposition (11), both of which are characteristics observed in aged muscle (70).

Natural advancement of age is associated with the gradual deterioration of immune system function, often referred to as immunosenescence (12). In fact, clinical observations indicate that elderly individuals are prone to severe, often lethal, infectious diseases following exposure to novel pathogens (71). Indeed, infections are more commonly encountered in the elderly and result in atypical clinical presentations, slow response to treatment and higher mortality rates (72, 73). Therefore, as aging is associated with a weakened immune response to disease, it is likely that the immune response to damaged skeletal muscle is likewise affected. In support of this assertion, studies of aged and undamaged human and animal muscle tissue show a significantly increased number of M2-like macrophages in the resident tissue (13, 17). Yet, in contrast, the tissue is often accompanied by elevated concentrations of several proinflammatory cytokines (eg, TNFα, IL-6) (13, 17, 74). These findings are particularly interesting when coupled with the findings of Brigitte et al, indicating that the resident macrophage population most likely directs the subsequent immune response following injury (75). Studies that have examined inflammatory cell behavior following skeletal muscle damage, particularly in an elderly population of humans, do not exist. Therefore, the aim of this study was to test the hypothesis that biological aging is associated with an abnormal accumulation of M2-like macrophages at rest and following skeletal muscle damage in humans. We further hypothesized that macrophage behavior with advanced age would affect myogenic capacity, such that aged myoblasts would demonstrate a more youthfullike potential when placed in a young macrophage environment. To test these hypotheses, we examined macrophage activity in vivo following an exercise-induced muscle-damaging protocol in young and old individuals. Additionally, we used a primary cell culture model to examine macrophage secretions and cell surface markers following incubation

in polarizing cytokines. We also examined the impact of young and old macrophage-conditioned medium on proliferation and differentiation potential of old human primary myoblasts.

Methods and Materials

Ethical Approval

Subjects were informed of all procedures and potential risks and signed a written, informed consent document approved by the Brigham Young University Institutional Review Board (Reference Numbers: F14529 and F17496). The study conformed to the standards set by the Declaration of Helsinki, except for registration in a database.

IN VIVO EXERCISE EXPERIMENT

Subjects

Eleven healthy young men and women (aged 22 ± 2 yrs, n = 11) and 8 old (aged 71 ± 7 yrs, n = 8) men volunteered to participate in this study, characteristics can be found in Table 2.1. The young group consisted of 7 men and 4 women. The old group consisted of all men. All subjects underwent a routine health questionnaire and screening. For the young group, physical activity ranged from sedentary to mildly active, but none was actively training in any particular sport, nor had they participated in a lower-body or upper-body strength training program for at least 6 months before participating in the study. For the old group, subjects were primarily screened on their ability to complete the exercise protocol. As a result, the old group was relatively more active. The old subjects reported regular participation in both aerobic and resistance training exercises throughout the week. Subjects were medication-free with the exception of one old subject who reported taking Lisinopril for high blood pressure and Pravastatin to lower cholesterol. All subjects agreed to refrain from participating in new physical activity or taking oral or topical analgesics for the duration of the study.

Study Design

The study consisted of four laboratory visits. Subjects reported to the laboratory on their first day and were familiarized to the Biodex dynamometer (Biodex Medical Systems, Shirley, NY). Muscle strength and soreness baseline measures were assessed and a preexercise control biopsy was taken from the vastus lateralis muscle of a randomized leg. At 24 hours after the preexercise biopsy, subjects returned to the lab to perform 300 maximal lengthening contractions on the leg opposite the randomized nonexercise leg. This protocol has been used by us and others to induce transient muscle damage (14-16, 30). Following completion of the muscle-damaging exercise, muscle strength and soreness were measured and subjects rested in the lab for 3 hours, after which a biopsy was taken from the vastus lateralis muscle of the exercised leg. The subjects then returned to the laboratory 24 hours and 72 hours postexercise to have muscle strength and soreness tested and to have muscle biopsies taken from the vastus lateralis muscle of the exercised leg.

Muscle Biopsy

Percutaneous needle biopsies were taken from the vastus lateralis muscle. The first biopsy was taken from the nonexercised leg before the exercise intervention. Three subsequent biopsies were taken at 3 hours, 24 hours, and 72 hours postexercise. Under local anesthesia (2% lidocaine), a small incision was made into the skin and fascia, and the biopsy needle was inserted into the muscle. With the use of manual suction, 75 to 150 mg tissue was withdrawn. Muscle samples were then separated from any fatty tissue, mounted on a cork with tragacanth gum and frozen in isopentane cooled in liquid nitrogen. Biopsy insertions that were performed on the same leg were placed 5 cm proximal to the last insertion to minimize potential confounding effects from previous biopsies (33). However, as samples were only taken from the exercised leg

postexercise, we cannot rule out that the observed changes may have been affected by repeated biopsies.

Assessment of Muscle Damage

Induction and assessment of muscle damage was performed as previously described (14, 15). Functional muscle capacity was measured on the Biodex dynamometer (Biodex Medical Systems, Shirley, NY). Before the strength trials, subjects were positioned so that their knee joints aligned with the axis of the dynamometer. The lever arm was then attached to their ankles 3 cm above the lateral malleolus. The positioning for each subject remained identical throughout the study. Isometric torque and impulse were measured at a knee joint angle of 70°. Subjects completed 3 maximal contractions of 5 seconds each with a 1-minute rest between each test. For every contraction, subjects were instructed to use as much force as possible in their motions. Consistent verbal encouragement was given for each repetition. Peak torque values were defined as the highest attainable value from the 3 trials, while impulse values were the calculated average for the duration of the contraction with an intraindividual coefficient of variation (≤ 5%).

Soreness was evaluated using a visual analog scale (VAS). We used a 100 mm line labeled from 0 mm to 100 mm with 0 mm indicating “no soreness” and 100 mm indicating “unbearable soreness.” Subjects were first instructed to perform 2 squats from a seated position. A chair was positioned behind each subject and adjusted so that contact with the chair was made at a knee flexion angle of 90°. During the task, subjects were asked to quantify the level of soreness experienced in the knee extensor muscles and mark the scale with a single vertical line accordingly. The distance from the left end of the scale to the mark was taken as the soreness level.

Immunohistochemistry

Eight-micrometer cross sections of muscle biopsy tissue samples were cut using a cryostat at −25 °C. Samples were mounted to Superfrost slides and air dried for 10 minutes. Slides were stained for proinflammatory (CD68/CD11b/dystrophin/DAPI) or anti-inflammatory (CD68/CD206/dystrophin/DAPI) macrophage markers or satellite cells (Pax7/DAPI). Sections were fixed in 2% paraformaldehyde (Sigma-Aldrich, St. Louis, MO) for 7 minutes. Following fixation, sections were washed 3 times in phosphate-buffered saline (PBS) solution for 3 minutes each. Sections were then blocked in 5% goat serum with 3% bovine serum albumin (BSA) solution for 60 minutes at room temperature in a humidified container. Sections were then incubated in the appropriate primary antibody overnight at 4°C. On the following day, samples were washed 3 times in PBS then incubated in the appropriate secondary antibody for 30 minutes at 37°C. Sections were again washed multiple times in PBS and rinsed in ultrapure water. Stained slides were then dried and mounted using Fluoroshield histology mounting medium (Sigma-Aldrich, St. Louis, MO). The following primary antibodies were used: CD68 mouse Monoclonal Antibody (eBioY1/82A (Y1/82A), eBioscience™ from Thermo Fisher Scientific, catalog # 14-0689-82, RRID AB_795874); CD11b mouse Monoclonal Antibody (1:100; deposited by T.A. Springer to Developmental Studies Hybridoma Bank, Iowa City, IA; LM2/1.6.11); CD206 mouse Monoclonal Antibody (1:100; deposited by Philip Stahl to Developmental Studies Hybridoma Bank, Iowa City, IA; MR Mab #46); Anti-dystrophin, rabbit polyclonal (1:100; Abcam: 15277,); Pax7 mouse Monoclonal Antibody (1:100; deposited by A. Kawakami to Developmental Studies Hybridoma Bank, Iowa City, IA; Pax7). Secondary antibodies used were: Cy™3 goat anti-mouse, IgG1 (1:100; Jackson ImmunoResearch Laboratories, West Grove, PA); Alexa Fluor® 488 goat anti-mouse, IgG2b (1:100; Jackson

ImmunoResearch Laboratories, West Grove, PA); Alexa Fluor® 647, goat anti-rabbit (1:100; Jackson ImmunoResearch Laboratories, West Grove, PA); DAPI (1:150; Thermo Scientific, Rockford, IL).

Quantification of Immunofluorescent Images

All quantification of immunofluorescent images was carried out by an investigator that was blind to both time point and subject grouping. For analyses, 1 to 6 (depending on the size of the sample) randomly acquired fields from each subject was imaged. For macrophage analysis, images were collected at each of the 4 time points, while satellite cell images were collected for the preexercise and 72-hour postexercise time points. Images were taken using a 20× objective and quantified using Olympus cellSens software.

To measure macrophage infiltration and activation, we assessed the immunoreactivity of mononuclear cells within the extracellular matrix of skeletal muscle. $CD68^{+}/DAPI^{+}$ cells were considered as a pan macrophage marker, whereas co-localization of $CD11b^{+}$ or $CD206^{+}$ cells were considered proinflammatory and anti-inflammatory macrophages, respectively (see Figure 1 for a representative image of general and polarized macrophages). Immunoreactivity of cells that were positive for $CD11b^{+}$ or $CD206^{+}$ and negative for $CD68^{-}$ were not considered as macrophages and were rarely located within the muscle sections. Therefore, quantification of proinflammatory and anti-inflammatory macrophages was determined by calculating the total number of proinflammatory or anti-inflammatory macrophages relative to the total number of macrophages. Additionally, quantification of macrophage and satellite cell ($Pax7^{+}/DAPI^{+}$) density was expressed relative to the total area of the imaged section. All analyses were done using Olympus cellSens software.

CELL CULTURE EXPERIMENTS

Blood Collection, Monocyte Isolation and Macrophage Maturation

Cell culture experiments were performed using human blood samples and a muscle biopsy sample of the vastus lateralis muscle. A diagram is presented in Figure 2. Human monocytes were collected and isolated using 70 mL of whole blood from 5 young and 5 elderly individuals. Briefly, peripheral blood samples were collected from the antecubital vein using a 21-gauge butterfly needle and 10 mL EDTA vacutainers® and subsequently diluted at a ratio of 1:1 in sterile PBS. Diluted blood samples were layered over Histopaque®-1077 (Ficoll) (Sigma, St. Louis, MO) solution, and peripheral blood mononuclear cells (PBMC's) were isolated via gradient centrifugation at 400 g for 20 minutes at room temperature with no braking. PBMC's were washed 3 times in PBS with EDTA then resuspended in serum-free attachment medium and seeded on tissue culture plates for 1 hour incubation at 37°C in 5% CO^2. Following attachment, cells were washed in sterile PBS to remove nonadherent cells, while the attached cells were suspended in monocyte maturation medium: RPMI-1640 supplemented with 10% fetal bovine serum (FBS) (Atlanta Biologicals, Flowery Branch, GA), 1% penicillin and streptomycin (Gibco, Waltham, MA) and 2 mM L-glutamine with 20 ng/mL GM-CSF (PeproTech, Rocky Hill, NJ). The monocytes were then incubated at 37°C in 5% CO^2 for 6 days, with medium being replaced every 72 hours. It should be noted that GM-CSF is shown to induce a proinflammatory phenotype, whereas the use of M-CSF directs maturation to more of an anti-inflammatory phenotype. In this study, mature macrophages treated with GM-CSF are used as the positive control.

Macrophage Polarization and Conditioned Medium

Mature macrophages were seeded at approximately 2.5 x 10^4 cells/cm^2 on 60 mm tissue-culture petri dishes and polarized/activated in their respective cytokine mediums for 24 hours. Medium consisted of RPMI-1640 with 2% FBS, 2 mM L-Glutamine (MØ) and either 20 ng/mL recombinant human Interferon-gamma (IFN-γ; PeproTech) plus 10 pg/mL lipopolysaccharide (LPS: Sigma; M1), or 10 ng/mL recombinant human interleukin-4 (IL-4: M2a; PeproTech), or 10 ng/mL recombinant human interleukin-10 (IL-10: M2c; PeproTech). To create cultured medium, activated macrophages were extensively washed in PBS and suspended in DMEM medium with 0.4% FBS, 1% Pen/Strep for 48 hours. After 48 hours the cultured medium (CM) was removed, centrifuged at 500 g for 5 minutes to remove cellular debris and frozen at −20°C.

Flow Cytometry

Once the mature macrophages had been polarized for 24 hours, the polarizing cytokine medium was decanted and cells were washed 3 times in PBS. Cells were then resuspended in 3 mL of Accutase (Sigma-Aldrich, A6964) and incubated at 37°C for 20 minutes. Following incubation, a cell scraper was used lightly to increase detachment of the cells from their respective plates before being transferred to 15 mL tubes. To ensure that the maximum number of cells were collected, each plate was washed twice with Flow Stain Buffer, which was added to the respective 15 mL tube. Cells were centrifuged at 400 g for 6 minutes at room temperature. The supernatant was then decanted, and each sample was resuspended in Human Fc receptor binding inhibitor (Invitrogen, 14-9161-73) and incubated for 15 minutes at 4°C. Next, conjugated primary antibodies were added to the cell solution: CD11b-FITC, CD206-PE, and CD163-APC and incubated at 4°C and protected from light for 60 minutes. Following incubation, 2 mL of Flow Stain Buffer was used to wash each sample before being centrifuged.

Cells were then resuspended in 500 µL of Flow Stain Buffer for analysis on the Beckman Coulter CytoFLEX cytometer (Brea, CA). The following antibodies were used in this experiment: CD206 (MMR) Monoclonal Antibody (19.2), PE, eBioscience™ from Thermo Fisher Scientific, catalog # 12-2069-42, RRID AB_10804655; CD11b Monoclonal Antibody (ICRF44), FITC, eBioscience™ from Thermo Fisher Scientific, catalog # 11-0118-42, RRID AB_1582242; and CD163 Monoclonal Antibody (GHI/61), APC from Thermo Fisher Scientific, catalog # A15723, RRID AB_2534503.

Cytokine Magnetic Bead Multiplexing Analysis

Cytokine content was measured using samples of our cultured medium. Briefly, cultured medium was obtained by extensively washing activated macrophages in PBS and suspending the cells in DMEM with 0.4% FBS for 48 hours, medium was collected and stored at −20°C. The Luminex Magpix multiplexing platform (Luminex xMAP Technology, San Diego, CA, USA) with a 13-plex magnetic bead kit (Cat#HSTCMAG28SPMX13) was used for multianalyte profiling of cytokine concentrations for each sample. In compliance with manufacturer's recommendations, antibody-conjugated magnetic beads were incubated with 25 µl of cultured medium overnight at 4°C on a plate shaker. Bead-complexes were then washed and incubated in detection antibodies for 1 hour on a plate shaker at room temperature. This was followed by incubation in streptavidin phycoerythrin for 15 minutes on a plate shaker at room temperature, with an additional 15-minute incubation in amplification buffer. Bead-complexes were resuspended in Assay Buffer and mixed on a plate shaker for 5 minutes, and then analyzed on a MAGPIX multiplex platform. Values are reported as pg/ml. Data were analyzed using Milliplex Analyst 5.1 software (Millipore Corporation, Billerica, MA, USA).

Culture of Human Primary Myoblasts with Macrophage-Conditioned Medium

Human primary myoblasts (HPM's) were collected from 5 healthy elderly (73.8 ± 5.8) individuals in accordance to previously published work (21) and approved by the Brigham Young University Institutional Review Board (Reference Number: F17496). After signing a written informed consent document, biopsies from the vastus lateralis muscle were collected, weighed, cut, and digested enzymatically (dispase II and collagenase D, Sigma) for 60 minutes at 37°C with titration every 15 minutes, then filtered and resuspended in growth medium. Cells were incubated at 37°C with 5% CO^2 for 7 days while changing the growth medium every 48 hours. After incubation, HPM's were isolated using Immunomagnetic Bead Sorting based on CD56 expression (miltenyi Biotec, 130-050-401), allowed to expand to approximately 70% confluency, and stored for later use in liquid nitrogen. This method has been shown to yield > 95% myogenic cell purity (21).

Myoblasts were pooled and seeded at 1.2 x 10^4 and 2.4 x 10^4 cells/well on 48 well-tissue culture plates coated with collagen (PureCol®, Advanced BioMatrix, Carlsbad, CA) for proliferation and differentiation assays, respectively, and run in duplicate. Seeding medium was removed after 24 hours and cells were washed in PBS and resuspended in conditioned medium for 24 hours (proliferation) or 72 hours (differentiation). Previous studies have shown that proinflammatory macrophages induce proliferation, while anti-inflammatory macrophages induce differentiation (9). Therefore, proliferation was examined using the conditioned medium of the IFN-γ/LPS-stimulated macrophages, while the IL-4-stimulated and IL-10-stimulated macrophages were used as the conditioned medium for testing differentiation. For both experiments, mature unstimulated macrophages where used as a positive control; untreated medium was used as a negative control.

Immunolabeling of muscle cells for proliferation and differentiation was performed following 24 hours and 72 hours of treatment, respectively. The 5-ethynyl-2'-deoxyuridine (EdU) was used to assess proliferation in accordance with Click-iT® EdU Alexa Fluor®488 Imaging Kit protocols (ThermoFisher Scientific). To assess differentiation, myosin heavy chain (MyHC) and myogenin expression were measured following 72 hours of incubation in conditioned medium. The 4',6-Diamidino-2-phenylindole dihydrochloride (DAPI) was used to measure total nuclei numbers. Specifically, at 72 hours, cells were fixed in 3% paraformaldehyde (PFA) for 2 minutes on a rocker, then permeabilized in 0.5% Triton® X-100 for 3 minutes, followed by another 2 minutes of fixation in 3% PFA. Cells were rinsed twice in phosphate buffered saline with 0.01% tween-20 (PBST) and then blocked in 3% BSA and 5% FBS for 30 minutes at room temperature. Cells were rinsed in PBS and incubated in the dark for 60 minutes on a rocker at room temperature in the respective primary antibodies (diluted in PBS at 1:100). Following 3 rinses in PBS, cells were then incubated with DAPI to stain nuclei and the appropriate secondary antibodies (diluted at 1:100 in PBS) for 60 minutes at room temperature in the dark. Lastly, cells were washed 3 times in PBS and images taken for analysis. Primary antibodies used were: Myogenin rabbit polyclonal M-225 (1:500; Santa Cruz Biotechnology: sc-576) and Myosin Heavy Chain mouse monoclonal antibody (1:500; deposited by D.A. Fischman to Developmental Studies Hybridoma Bank, Iowa City, IA; MF-20). Secondary antibodies used were: Alexa Fluor® 488, goat anti-mouse (1:100; Jackson ImmunoResearch Laboratories, West Grove, PA); Cy3®, goat anti-rabbit (1:500; Jackson ImmunoResearch Laboratories, West Grove, PA); and DAPI (1:1000; Thermo Scientific, Rockford, IL)

Imaging and Analysis

Three random sample images of 578 ± 44 cells per image were collected from each well by investigators that were blind to both group and treatment using an Olympus IX73 microscope and Olympus XM10 camera. Proliferation was analyzed after 24 hours in conditioned medium by counting the number of EdU^+ nuclei, expressed as a ratio of total nuclei. Differentiation was measured after 72 hours of incubation in conditioned medium by comparing the number of $Myogenin^+$ nuclei to total nuclei. Furthermore, total myotube area was measured by the expression of MyHC. Nuclei within the MyHC area were counted and expressed as a percentage of total nuclei-differentiation index. Images were analyzed using Olympus cellSens™ microscope imaging software. Additionally, time lapse images were collected every 15 minutes for 6 days using the Lonza CytoSMART™System (Lonza) to analyze muscle cell proliferation with young macrophage-conditioned and old macrophage-conditioned medium.

Statistics

A repeated measures mixed model analysis with main effects for group, sex, and time were used in conjunction with the interaction of group × time to test functional data, macrophage phenotype and satellite cell number. The covariate of body mass index (BMI) was added to the model for assessing functional data. A student's t-test was performed post hoc when the fixed-effect test revealed a significant p-value for a main effect or the group × time interaction. For macrophage polarization using flow cytometry, cytokine response data and cell culture experiments, a mixed model ANOVA was used to detect differences between age groups and treatments. Post hoc analysis of the group × treatment interaction was used to test differences between age groups for each treatment protocol. To normalize distributions and homogenize variance, the following variables were log-transformed; Soreness, GM-CSF, IFN-y, TNFα, IL-2,

IL-4, IL-6, IL-7, IL-10, IL-12(p40), IL-13, yet are presented as absolutes. Prism Graphpad (V6.0b; San Diego, CA, USA) was used to create figures. JMP® Pro (V12.2; SAS Institute, Cary, NC, USA) was used for all statistical analysis. Data are presented as means ± SD Results were considered statistically significant at $p < 0.05$.

Results

Subject Characteristics

Subject characteristics can be found in Table 2.1. As this cohort of subjects was used in a previously published study, exercise performance data, muscle fiber characteristics and assessment of muscle damage can be found in that manuscript (14).

Macrophage Response

Immune cell infiltration, especially macrophages, are a critical component of healthy muscle repair and adaptation (65, 76). Analysis of the total ($CD68^+/DAPI^+$) macrophage population following a bout of muscle-damaging exercise showed a similar overall increase in macrophages between young and old subjects, which peaked at 72 hours postexercise (young: 4326 ± 2622 vs old: 5287 ± 2248 cells/mm^3, time: $p = 0.001$) (Figure 2.3A). Furthermore, proinflammatory $CD11b^+/CD68^+/DAPI^+$ macrophages also showed a similar time response between young and old groups, peaking at 24 hours (young: 2814 ± 2020 vs old: 2991 ± 2712 cells/mm^3) (Figure 2.3B). However, when calculated as a ratio ($CD11b^+/CD68^+/DAPI^+$ to $CD68^+/DAPI^+$ cell/mm^3), we detected a significant group × time interaction, such that post hoc analysis revealed a significantly higher proportion of proinflammatory macrophages at 24 hours postexercise in the young individuals (young: 75 ± 15 vs old: 53 ± 18%, $p = 0.027$) (Figure 2.3C).

Anti-inflammatory macrophage analysis confirmed a similar increase in $CD68^{+}/DAPI^{+}$ macrophages between young and old, as was previously reported for the proinflammatory macrophage analysis, peaking at 72 hours (young: 5537 ± 2711 vs old: 5328 ± 1624 cells/mm^3, time: $p = 0.001$) (Figure 2.3E). Likewise, anti-inflammatory $CD206^{+}/CD68^{+}/DAPI^{+}$ macrophages also peaked at 72 hours postexercise (young: 2890 ± 1720 vs old 4066 ± 916 cells/mm^3, time: $p = 0.037$). We observed a significant main effect for age group ($p = 0.0037$), such that the overall number of anti-inflammatory $CD206^{+}/CD68^{+}/DAPI^{+}$ macrophages was greater in the old across all time points (Figure 2.3F). When calculated as a ratio ($CD206^{+}/CD68^{+}/DAPI^{+}$ to $CD68^{+}/DAPI^{+}$ macrophages), this finding was confirmed, showing that the overall proportion of anti-inflammatory macrophages was greater in the old (group: $p = 0.0005$). Additionally, it revealed that the greatest decline in the proportion of anti-inflammatory macrophages took place at 24 hours postexercise in both the young and old (young: 36 ± 13 vs old: 64 ± 18%, time: $p = 0.002$) (Figure 2.3G).

An unexpected finding from our study was the appearance of a rare subset of cells ($CD11b^{+}/CD68^{-}/DAPI^{+}$) in the old. An example image can be found in Figure 2.4C. A portion of the elderly subjects displayed an atypical accumulation of this cell type at 24 hours postexercise (young: 238 ± 264 vs old: 2671 ± 3065 $CD11b^{+}/CD68^{-}/DAPI^{+}$ cells/mm^3, $p = 0.063$) (Figure 2.4A). Interestingly, we observed that the infiltration of these atypical cells strongly correlated ($r2 = 0.79$, $p = 0.0031$) (Figure 2.4B) with intramuscular IL-8 concentrations that were measured in the same subjects and published as a separate investigation (14), indicating that the cells may be neutrophils. However, we are unable to draw specific conclusions from the current data since other cell types, such as eosinophils, have also been shown to express CD11b. No differences

were detected in the extremely rare appearance of $CD206^{+}/CD68^{-}/DAPI^{+}$ cells (data not presented).

Satellite Cell Response

Satellite cell content was measured by counting the number of $Pax7^{+}/DAPI^{+}$ cells per volume of muscle tissue (cross-sectional area • section thickness (8μm)) (60), and representative images can be found in Figure 2.5. We found satellite cell content to be similar between young and old subjects at the preexercise time point (young: 137 ± 51 vs old: 150 ± 33 cells/mm^3, p = 0.4). However, at 72 hours following the bout of muscle-damaging exercise, we measured a significant increase in satellite cell content in the young (181 ± 41 cells/mm^3, p = 0.015), while no change was observed in the old (137 ± 39 cells/mm^3, p=0.5) (Figure 2.5D).

Flow Cytometry

Previous studies suggest that aged macrophages are less capable of responding to various stimulating cytokines. Therefore, we used flow cytometry as a means to test the sensitivity of young and old macrophages to transition from a proinflammatory to an anti-inflammatory phenotype following 24 hours of cytokine stimulation (Figure 2.6). Macrophages were stimulated with either IL-4 or IL-10 to induce M2 polarization. As expected, we detected a significant main effect for treatment, such that the percentage of CD206 and CD163 positive cells were elevated in both young and old groups when treated with IL-4 and IL-10, respectively (Figures 2.6 C-E). In other words IL-4 and IL-10 treatments both induced an M2-like response in our otherwise proinflammatory macrophages. Moreover, we also found that the percentage of cells with the cell surface markers CD206 and CD163 (shown in quadrant 3) were significantly greater in the old compared to the young following IL-10 treatment (young: 3.7 ± 2 vs old: 18.8

± 19%, p = 0.0021), suggesting a stronger propensity of old macrophages to adopt an M2 phenotype in response to IL-10 (Figure 2.6D).

Cytokine Magnetic Bead Multiplexing

To test the hypothesis that old macrophages secrete fewer cytokines than young macrophages in response to a targeted polarization stimulus, secreted cytokine concentrations were measured in macrophage-conditioned medium of young and old individuals using a 13-panel multiplexing magnetic bead assay. Mature macrophages were treated with either IFN-γ/LPS to induce a proinflammatory response or IL-4 or IL-10 to induce an anti-inflammatory response. Conditioned medium from nonpolarized macrophages was used as a positive control. We detected an increase of proinflammatory cytokines GM-CSF, IFN-γ, TNFα, IL-6, IL-7, and IL-12 for the cells treated with IFN-γ/LPS, indicated by a significant treatment effect (Figure 2.7). Likewise, there was a significant treatment effect for cells polarized to an anti-inflammatory phenotype, as indicated by the increase in IL-4 and IL-10. As IL-13 is known to have anti-inflammatory properties, we were surprised to see an increase in IL-13 in the IFN-γ–treated macrophages. We also detected age group differences for IFN-γ, IL-7 and IL-13, demonstrating that the cumulative concentration for each respective secreted cytokine was greater in the young group across treatments. Furthermore, we found that the control group (mature macrophages that were not treated with polarizing cytokines) had significantly higher concentrations of GM-CSF, IFN-γ, IL-7 and IL-13 in the young group relative to the old. Of particular interest were the cytokines that have been shown to influence satellite cell behavior, these include TNFα and IL-6 (9). When treated with INF-y, TNFα (young: 122 ± 149 vs old: 27 ± 14 pg/ml, p = 0.0092) and IL-6 (young: 61 ± 132 vs old: 0.84 ± 0.9 pg/ml, p = 0.047) were markedly greater in the young,

along with IL-7 and IL-12 (p40). Treatment with IL-4 resulted in a similar cytokine response between young and old, while only IL-7 was greater in the young for the IL-10 treatment.

Myoblast Proliferation and Differentiation

Macrophages have been shown both in vitro and in vivo to facilitate satellite cell behavior. In particular, proinflammatory macrophages secrete cytokines that influence satellite cell proliferation, while anti-inflammatory macrophages direct differentiation (9). To test the hypothesis that a young macrophage environment could rejuvenate old myoblasts, we used macrophage-conditioned medium from cells treated with IFN-γ/LPS to test myoblast proliferation. For differentiation, anti-inflammatory-conditioned medium was collected from cells treated with IL-4 or IL-10. In both experiments, mature macrophages that were not polarized were used as a positive control, and unconditioned medium was used as a negative control. We found that macrophage-conditioned medium improves both proliferation and differentiation of human primary myoblasts (HPM's) when compared to unconditioned medium alone (Figure 2.8). Furthermore, aged HPM's treated with young macrophage-conditioned medium increased their proliferative capacity by an average of 32% when compared to HPM's treated with old macrophage-conditioned medium (Figure 2.8A). We also found that myotube area and differentiation index were greater overall when treated with young macrophage-conditioned medium relative to medium conditioned by old macrophages, indicated by a significant age group effect, especially when treated with IL-4. However, no differences between young macrophage-conditioned and old macrophage-conditioned medium were detected for the expression of myogenin (Figure 2.8B-D).

Discussion

Macrophages are the most plastic and complex of the immune cells found throughout the body. Macrophages act as first responders to identify and fight off infection and influence complex cell to cell interactions to repair damaged tissue. However, studies show that with age, immune cells, including macrophages, become less responsive and dysfunctional, especially in protecting against invading pathogens (12, 71). Furthermore, animal studies show that macrophages present an abnormal anti-inflammatory phenotype in old skeletal muscle, which can negatively influence skeletal muscle quality (17, 19). Therefore, the primary aim of the current study was to investigate the acute (up to 72 hours) inflammatory (macrophage) response in skeletal muscle of healthy young and elderly humans following a bout of damaging exercise. Consistent with our hypothesis, we found that skeletal muscle of older (mean age 70.9 ± 7.3 years) individuals displayed a reduced M1 and amplified M2 macrophage response relative to young individuals following exercise-induced muscle damage. Further, in vitro experiments using primary monocyte and myoblast cultures showed that the macrophage population of older subjects displayed a greater propensity to take on an M2 phenotype as indicated by the appearance of cell surface marker CD163 (flow cytometry), suggesting greater sensitivity to IL-10 stimulation. Conversely, macrophages collected from the older population secreted significantly less cytokines than macrophages from the young group, especially cytokines that are considered to be proinflammatory, indicating a reduced capacity to respond to cytokine treatments that induce an M1 phenotype. Finally, incubating old myoblasts in young, polarized macrophages improved proliferation, and, in some cases, differentiation, suggesting that just as macrophages from older individuals are less responsive to infection, they are less capable of stimulating processes of repair in skeletal muscle tissue.

This is the first study to comprehensively investigate macrophage activity following a protocol designed specifically to induce nonpathological muscle damage in aged humans. To study the muscle inflammation response in humans, we used a lengthening contraction paradigm of muscle damage. The inflammatory response following this type of exercise stress has been well documented in young individuals (41). Others have shown that it results in a robust infiltration of macrophages, which peak between 2 and 3 days postexercise (13, 16). However, the time course of macrophage polarization has yet to be comprehensively investigated in this model. Consistent with many of the animal damage models, we show that infiltration of M1-polarized ($CD11b^+/CD68^+/DAPI^+$) macrophages peak at around 24 hours postexercise, whereas M2-polarized macrophages ($CD206^+/CD68^+/DAPI^+$) are more abundant at the later 72-hour time point. We also observed that total $CD68^+/DAPI^+$ macrophage infiltration was similar between young and old groups. Importantly, we found that the aged population did not mount as strong of a proinflammatory response as the young at the 24-hour M1 peak following the exercise. This is apparent by the decreased proportion of macrophages expressing the proinflammatory marker CD11b. In support of this finding, Przbyla et al also found that proinflammatory macrophages increased in young, but did not change in old individuals 72 hours following a resistance exercise protocol (13). Conversely, our previous findings show that MCP-1, the chemokine responsible for recruiting macrophages to the site of tissue damage and typically characteristic of a proinflammatory response, was significantly elevated in the muscle tissue of older subjects when compared to young (14). Taken together, these data suggest that aged macrophages may have an impaired capacity to respond to proinflammatory stimuli. In fact, Herrero et al showed that macrophages treated with interferon-gamma (IFN-γ), which can induce the proinflammatory macrophage phenotype in skeletal muscle, expressed 50% less of the MHC class II complex in

old mice, a classical proinflammatory marker (77). Unfortunately, we were unable to detect cytokines associated with proinflammatory macrophage polarization (IFN-γ and TNFα) in our muscle tissue samples. Nonetheless, our cell culture assay supports this idea, as we measured markedly less proinflammatory cytokine concentrations in the old for macrophages treated with IFN-γ. Indeed, a dampened proinflammatory response in skeletal muscle would likely result in undesirable complications for healthy tissue repair due to the responsibilities associated with healthy muscle regeneration and macrophage activation. These include phagocytosis and clearing of dead cells and debris, secretion of enzymes that break down the extracellular matrix, and the stimulation of various cellular functions such as proliferation and apoptosis of satellite (9), and fibro-adipogenic progenitor (FAP) (11) cells, respectively (12).

As hypothesized, we also observed an overall tendency for aged macrophages to present an anti-inflammatory phenotype. This is evident by the increased number and proportion of macrophages that were positive for the CD206 marker. This finding is consistent with previous studies in humans (13, 78) and animals (17) that likewise show an elevated anti-inflammatory phenotype in macrophages both at rest and following resistance exercise or disuse in aged muscle. Interestingly, as it is generally accepted that aged muscle is less capable of adaptation and repair, these findings appear contradictory to what one might expect, based on the regenerative role of anti-inflammatory macrophages in skeletal muscle. Nevertheless, an elevated or untimely transition to an anti-inflammatory macrophage phenotype is characteristic of other skeletal muscle pathologies such as muscular dystrophy, which predispose the tissue to reductions in function and quality (11). Indeed, there is accumulating evidence showing the influence of the immune system in regulating skeletal muscle quality, growth and regeneration in both acute and chronic muscle injury models due to the important source of cytokines and other

secreted factors that immune cells produce (9, 79). Results from our current study, as well as others, support the idea that anti-inflammatory macrophages promote proliferation and differentiation of satellite cell populations (65, 80). Thus, our observation of an increase in satellite cell content in only the young at 72 hours postexercise, despite an age-related increase in anti-inflammatory macrophages, is somewhat contradictory to this theory and would suggest that more complex interactions take place in the skeletal muscle as compared to cell culture experiments. Indeed, it also suggests that we often determine cellular outcomes based on generalized phenotypical markers, when, in reality, functional measures should be used as a more conclusive indicator of cell behavior.

An unexpected finding in the tissue samples of older subjects was the accumulation of $CD11b^{+}/CD68^{-}/DAPI^{+}$ cells 24 hours postinjury in a portion of the older samples. Though the data did not reach statistical significance, likely due to subject variability and sample size, this aggregation of cells was clearly distinguishable from other time points and portions of the tissue sample. Specifically, these cells appeared in more dense sections of the extracellular matrix, possibly described as the perimysium or in areas of greater fiber damage (see Figure 4) (81). Other than proinflammatory macrophages, CD11b is expressed on the surface of several leukocytes including monocytes, neutrophils and granulocytes. Though we are uncertain as to the cell population that is present in these individuals, it is interesting to note that our previous study showed a significant elevation of intramuscular IL-8, a chemokine associated with neutrophil chemotaxis, 24 hours following the bout of damaging exercise in the same individuals. Indeed, controversy surrounding neutrophil activity exists in the literature, as previous studies have linked neutrophils with exacerbated muscle damage (81), while others show that neutrophil accumulation promotes adaptation and quicker recovery of strength (82). Our data is more

representative of an adaptation that improved strength restoration, yet the data is insufficient to make clear conclusions, as these cells were only observed in the old. A recent study by Sloboda et al hypothesized that neutrophil accumulation would persist in old mice following a bout of LC's, yet observed a similar rise and fall in neutrophil numbers at 2 days and 5 days postexercise. However, the overall presence of neutrophils was greater in the old when compared to the young (83). When considered in the context of these animal studies, our data suggest that aged muscle appears to have an atypical immune-cell response both at rest and following exercise-induced muscle damage. Indeed, the greater proportion of anti-inflammatory macrophages coupled with the accumulation of other immune cells in old muscle indicate a need for future studies to examine a more complete immune-cell response following injury.

Based on our in vivo findings, we conducted several cell culture experiments to identify potential mechanisms that might help explain why aged macrophages have a greater anti-inflammatory phenotype, and to investigate how abnormal macrophage behavior might contribute to the age-related decline in muscle repair. To do this, we examined cytokine secretions and cell surface markers associated with proinflammatory and anti-inflammatory macrophages following activation in polarizing cytokines. We also measured the impact of young and old macrophage-conditioned medium on aged myoblasts. Treatment with IFN-γ/LPS was considered as an M1, proinflammatory, stimulator, while anti-inflammatory, M2, macrophages were induced via IL-4 and IL-10. As hypothesized, our primary finding was that human primary myoblasts (HPMs) are more responsive to macrophage-conditioned medium, especially when placed in a young-macrophage environment. This was evident by the increased number of EdU^+ cells in myoblasts treated with young macrophage-conditioned medium, as well as the significant effect for age group in myotube formation and differentiation index. We

believe that our cytokine assay supports this finding, as IL-6, which has been shown to increase myoblast proliferation (9), was elevated in the young. Furthermore, a recent study by Wang et al performed a similar experiment using young macrophage-conditioned and old macrophage-conditioned medium from mice to test proliferation and differentiation of C_2C_{12} cells. They showed increased proliferation in the young based on Ki67 and MyoD expression, as well as greater differentiation based on myogenin expression, where we did not find differences in myogenin. A possible explanation for this discrepancy may be that their cell maturation protocol involved incubation of bone marrow cells in M-CSF, which is thought to induce an anti-inflammatory phenotype, while we used GM-CSF, which has been shown to induce a more proinflammatory phenotype (19). As such, it is possible that their population of macrophages were more developed to a phenotype that would promote differentiation and make it more likely to detect differences. Furthermore, we measured myogenin expression at the protein level, whereas Wang et al measured gene expression using PCR. Lastly, the use of primary human myoblasts and macrophages likely represent a more genetically diverse population of cells than C_2C_{12} cells and immune cells collected from interbred animals. However, in support of their findings, we did detect group differences for differentiation, measured by the formation of myotubes and differentiation index, especially with IL-4 treatment. However, as we were unable to detect differences between young and old samples for cytokines related to an anti-inflammatory phenotype, specifically, IL-4 and IL-10, it is possible that anti-inflammatory macrophages respond normally in old humans. In fact, the accumulation of anti-inflammatory macrophages in aged skeletal muscle suggests that aged macrophages are more capable of performing anti-inflammatory functions. This was further supported in our previous work, which showed a premature activation of the TGF-β family of proteins in the old subjects following the

bout of damaging exercise. However, as TGF-β concentrations where measured in the whole tissue sample, we cannot make clear conclusions about its secretion from anti-inflammatory macrophages. Interestingly, studies have shown that proinflammatory and anti-inflammatory macrophages use differing metabolic pathways. Proinflammatory macrophages are more reliant on the glycolytic energy pathway whereas anti-inflammatory macrophages rely on oxidative energy production (84), suggesting that the capacity to transition from one phenotype to another can be lost in one direction and preserved in the other. Therefore, future studies may seek to examine more closely the anti-inflammatory functions of aged macrophages.

Lastly, we observed that aged macrophages displayed an increased sensitivity to the IL-10 treatments, indicated by the increased percentage of cells that were positive for CD163. Previous studies have shown that aged muscle is characterized by a general increase in IL-10 levels (13, 17), with those same studies reporting an increased percentage of anti-inflammatory macrophages in older muscle tissue (13, 17). Taken together, it is possible that the accumulation of anti-inflammatory macrophages in the old is attributed to the increased availability and sensitivity of IL-10. Conversely, Mahbub et al measured significantly fewer IL-4 receptors on the macrophages of aged animals (85), which is in contrast to what we would expect. Nonetheless, as IL-10 is also a potent activator of the anti-inflammatory phenotype, typically identified by the expression of the cell surface marker CD163, it would be interesting to examine the appearance of the IL-10 receptor on macrophages of aged humans. Furthermore, a recent study by Akahori et al discovered a physiological role for CD163 (86), which may explain how an abnormal increase in anti-inflammatory macrophages may attenuate successful satellite cell activity. Acting as a decoy receptor for TWEAK signaling and subsequent notch activation, CD163 binds TWEAK to induce myogenic differentiation of satellite cells, suggesting that

elevated or early onset of anti-inflammatory macrophages may attenuate satellite cell proliferation and induce premature differentiation, resulting in delayed and incomplete muscle repair.

In conclusion, we have shown that aged skeletal muscle is associated with an irregular accumulation of anti-inflammatory macrophages and $CD11b^{+}/CD68-$ cells in response to muscle-damaging exercise, possibly as a result of increased sensitivity to IL-10. Furthermore, we have provided evidence to suggest that aged macrophages release fewer cytokines in response to polarizing stimuli, which may help explain why myoblasts proliferate, and in some cases differentiate, at a faster rate in young macrophage-conditioned medium. As this is the first study to comprehensively investigate aging and macrophage polarization in human skeletal muscle using a nonpathological muscle-damaging model, we believe that it adds value to the current understanding of skeletal muscle adaptations that occur with age. Indeed, the creation of therapeutic or pharmacologic interventions that target healing of skeletal muscle tissue, particularly in the elderly, would provide immediate clinical value to the rapidly increasing population of elderly individuals that suffer from complications related to muscle injury.

Table 2.1. Subject Characteristics

Group	Age (years)	Sex	Height (cm)	Weight (kg)	BMI, kg/m^2
Young (n = 11)	22.2 ± 2.2	Males (7) Females (4)	174.3 ± 7.5	76.3 ± 14.7	25.1 ± 4.7
Old (n = 8)	70.9 ± 7.3	Males (8)	175.3 ± 6.8	88.1 ± 15.1	28.6 ± 4.3

Notes: Data are means ± SD; BMI, body mass index.

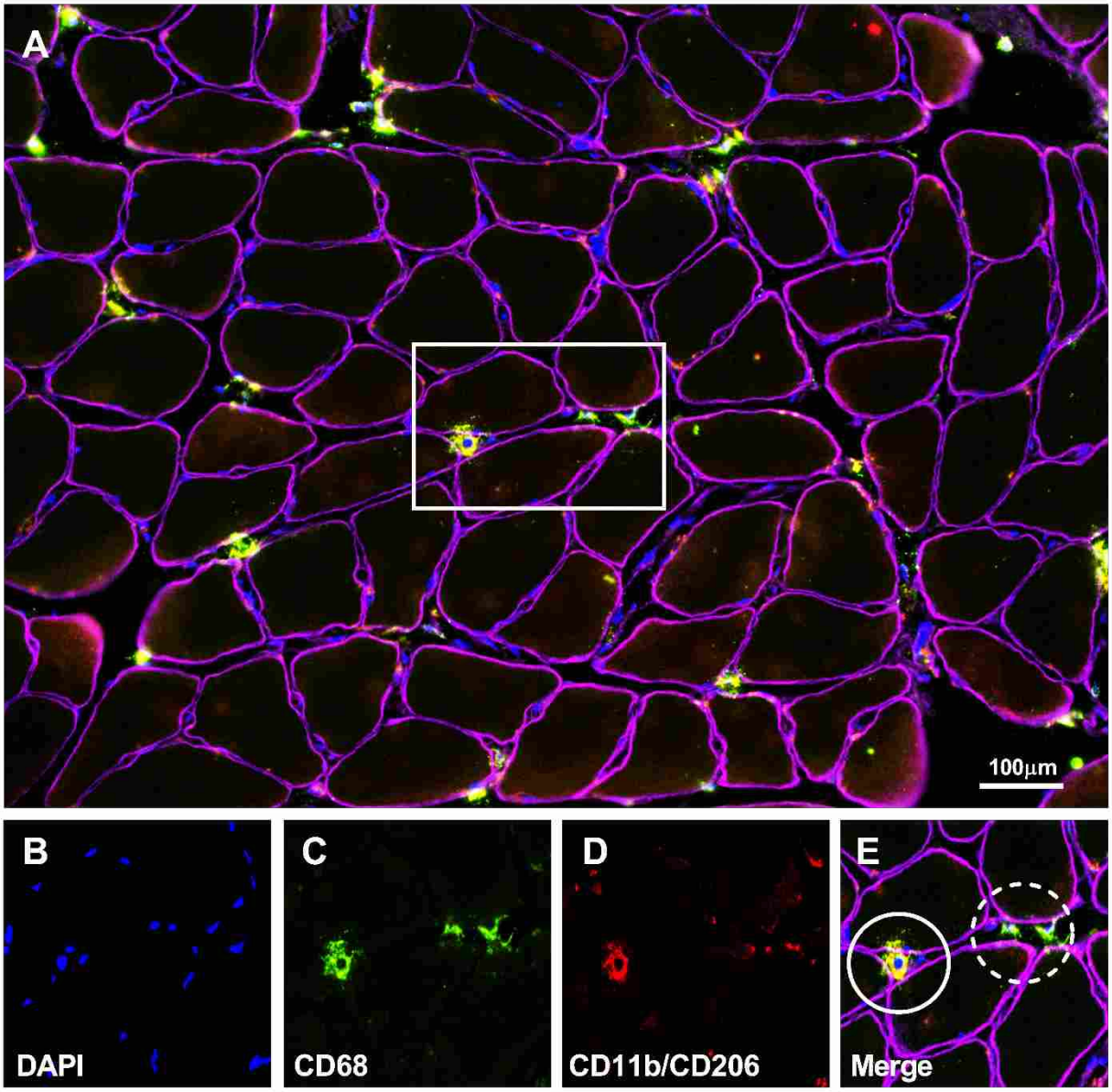

Figure 2.1: Macrophage Analysis. (A) Representative image of immune cell infiltration to skeletal muscle following a bout of muscle-damaging exercise. The solid white rectangle located within image A is further depicted in images B-E. **(B)** DAPI (blue) was used as a marker for nuclei. **(C)** CD68 (green) was used as a pan macrophage marker. **(D)** CD11b (proinflammatory) or CD206 (anti-inflammatory) (red) were used to identify activated/polarized macrophages. **(E)** Dystrophin (purple) was used to identify the muscle fiber membrane and to ensure that macrophage cells were located within the extracellular matrix. The solid white circle in image E represents a polarized macrophage with colocalization of CD68 and CD11b or CD206 with DAPI, while the dotted white circle represents pan macrophages CD68/DAPI.

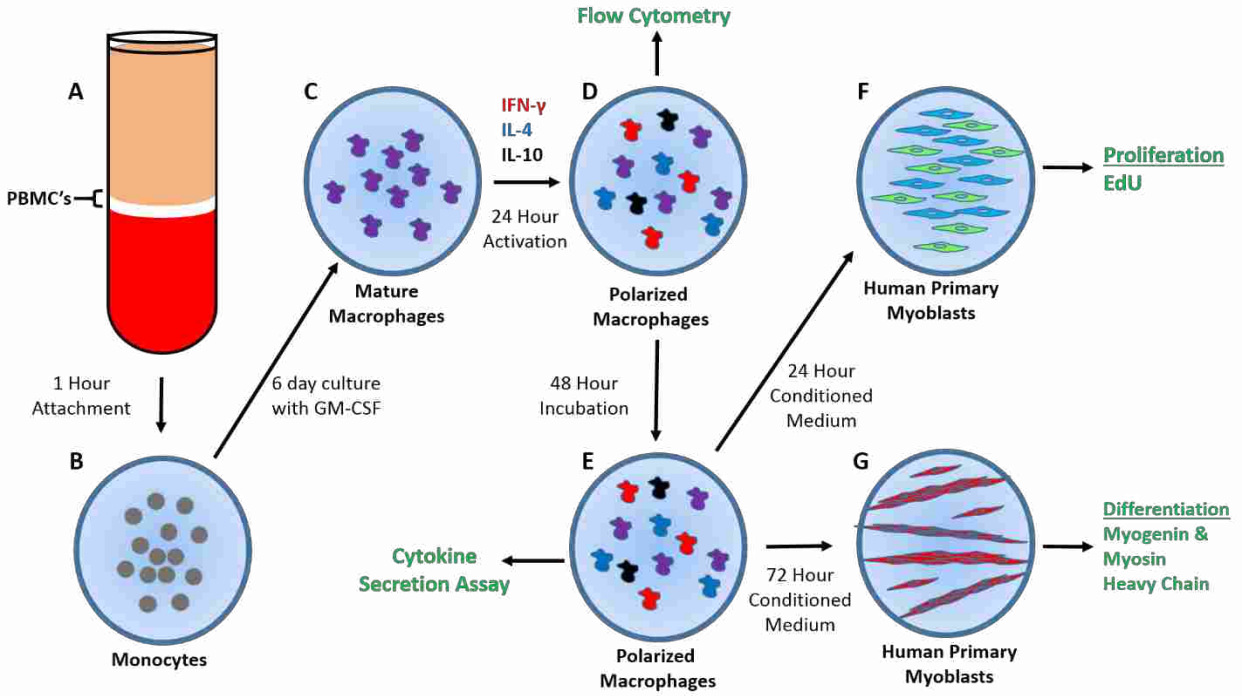

Figure 2.2: Cell Culture Study Design. (A) Peripheral blood mononuclear cells (PBMC's) were collected from 5 young and 5 old individuals and **(B)** monocytes were isolated via cell attachment. **(C)** Cells were incubated for 6 days to allow monocytes to mature into macrophages and then **(D)** activated/polarized for 24 hours, after which a portion of the cells were tested using flow cytometry. **(E)** The remaining cells were suspended in DMEM for 48 hours to produce the conditioned medium, then the cells were tested using flow cytometry. Conditioned medium was examined for secreted cytokine concentrations and also added to myoblast cultures to test **(F)** proliferation and **(G)** differentiation potential. IFN-γ: interferon-gamma, IL-4: interleukin-4, IL-10: interleukin-10. Purple = M0 macrophage, Red = M1 macrophage, Blue = M2a macrophage, and Black = M2c macrophage. Green = time and type of analysis performed.

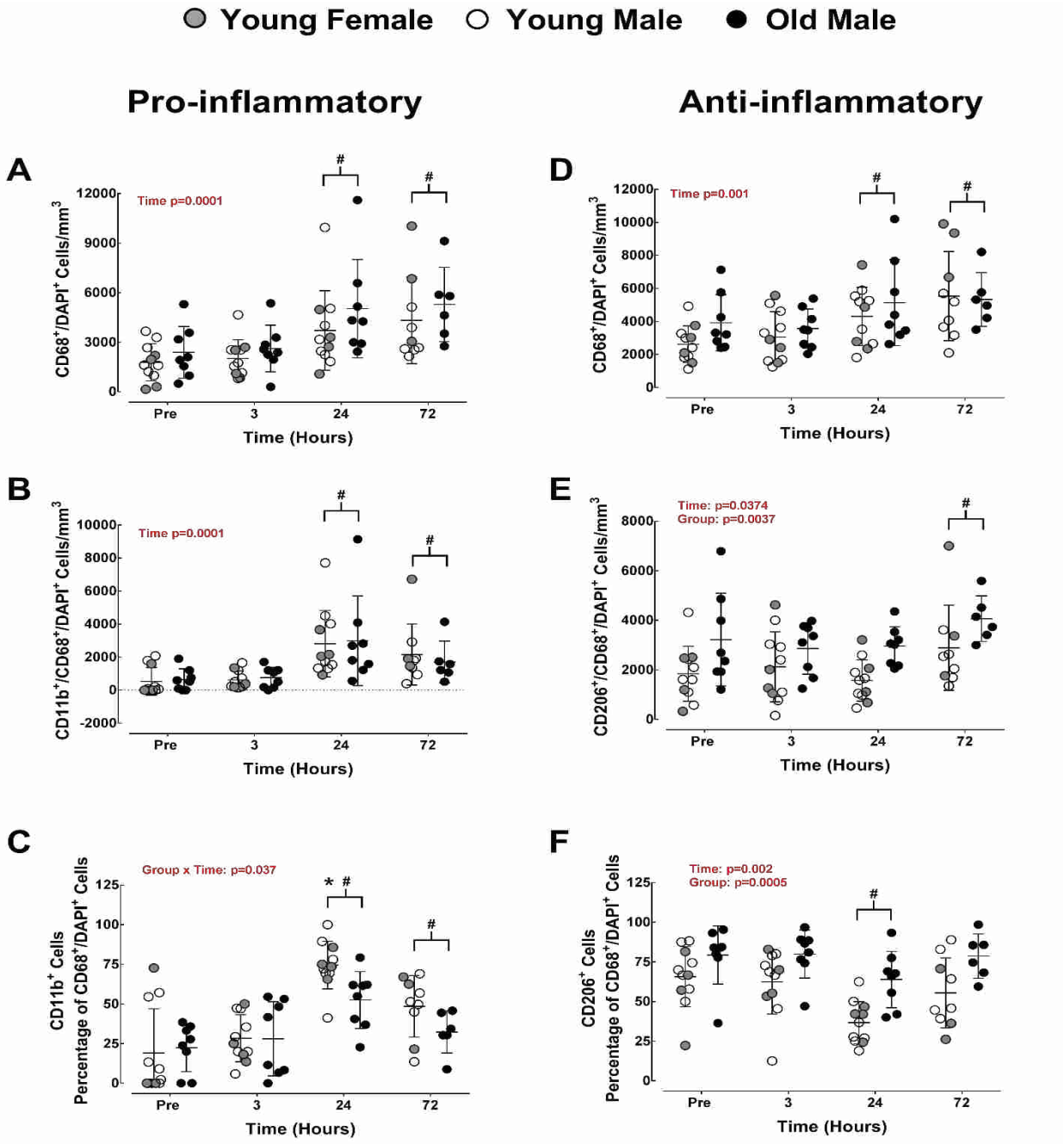

Figure 2.3: Macrophage Data. The **(A, D)** infiltration and activation of proinflammatory **(B, C)** and anti-inflammatory **(E, F)** macrophages in skeletal muscle were measured at baseline and at 3 hours, 24 hours, and 72 hours following a bout of muscle-damaging exercise. Data are presented as mean ± SEM for the number of cells/mm^3. #Significantly different from baseline. *Significantly different between young and old groups. Significance set at $p < 0.05$.

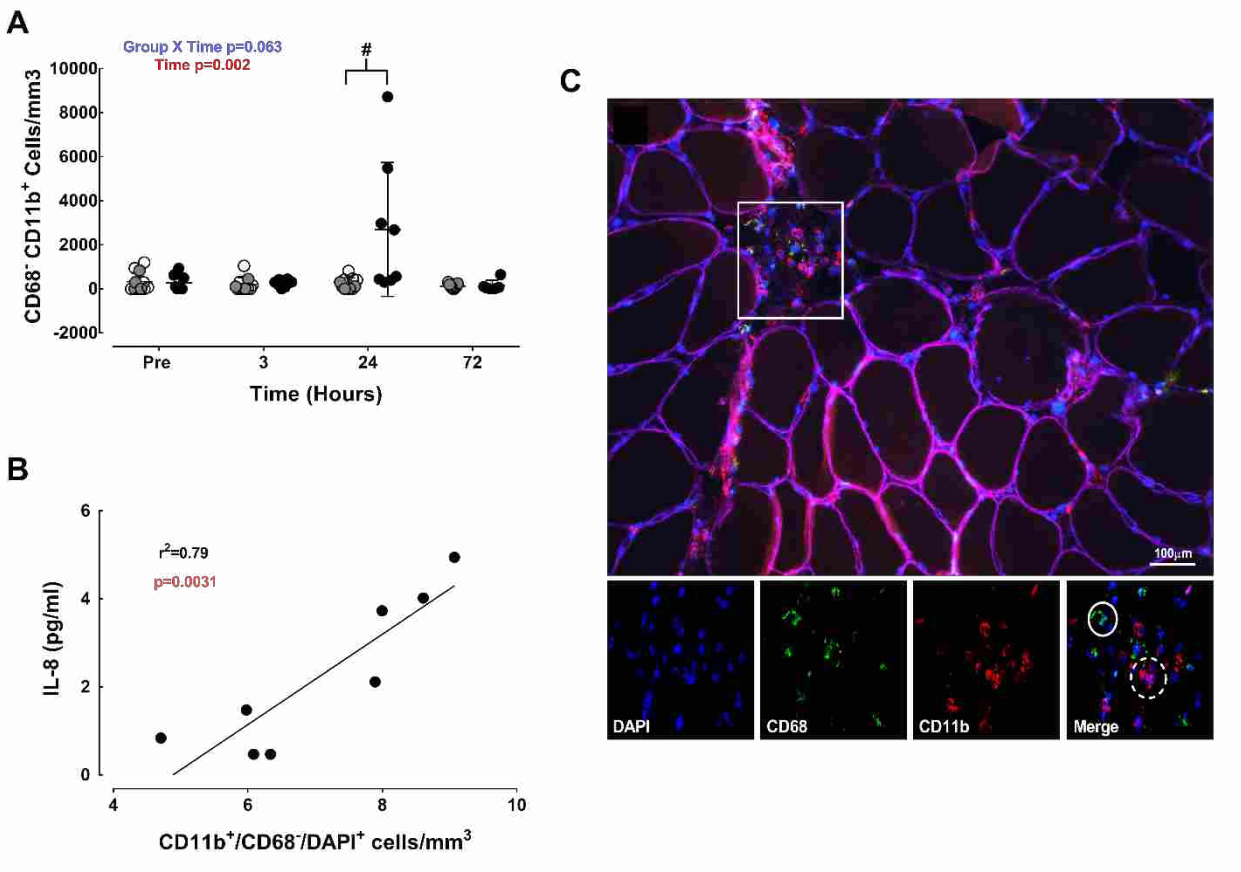

Figure 2.4: CD68^{-}/CD11b^{+}/DAPI^{+} Immune Cells. (A) A rare population of cells that stained positive for CD11b and negative for CD68 appeared in a portion of old subjects 24 hours following the bout of muscle-damaging exercise and had a strong correlation **(B)** with intramuscular IL-8 expression of old subjects. **(C)** Representative image 24 hours following the bout of exercise that shows pooling of immune cells in the extracellular matrix of an old subject. The solid white square is represented in the images below, indicating the different cell populations. DAPI (blue) was used to mark nuclei. CD68 (green) is a pan macrophage marker. CD11b (red) stained for proinflammatory macrophages and a subset of immune cells. Dystrophin (purple) represents the muscle fiber membrane. The solid white circle depicts a macrophage while the dotted white circle represents an immune cell other than a macrophage. This cell population is likely representative of neutrophils. Data are presented as mean ± SD for the number of cells/mm^3. #Significantly different from baseline. Significance set at $p < 0.05$.

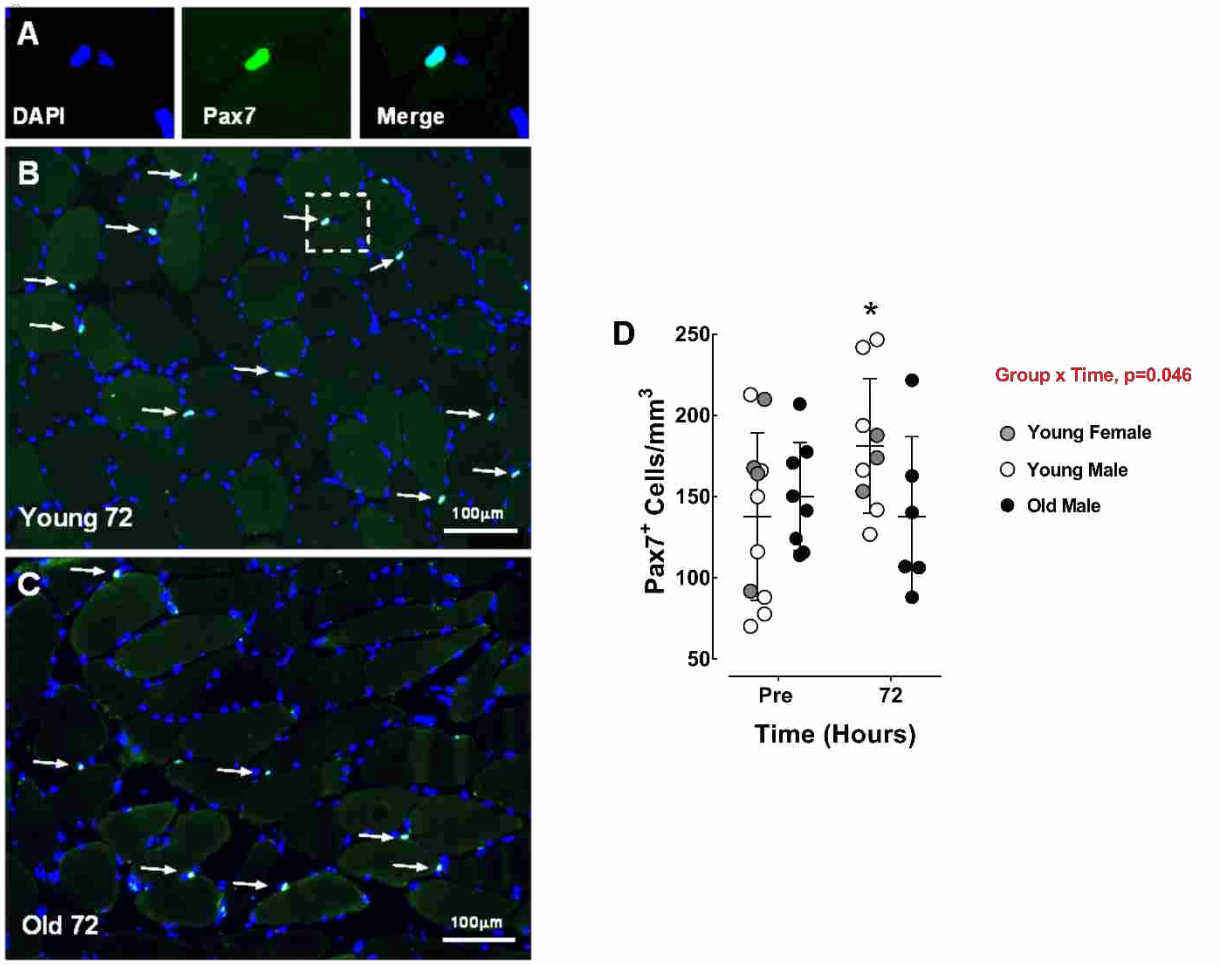

Figure 2.5: Satellite Cells. (A) Representative images of nuclei (blue) and satellite cells (green) in **(B)** young and **(C)** old subjects 72 hours following a bout of muscle-damaging exercise. Satellite cell data is presented as means ± SD for the number of $Pax7^+$ cells/mm^3. *Significantly different between young and old groups. Significance set at $p < 0.05$.

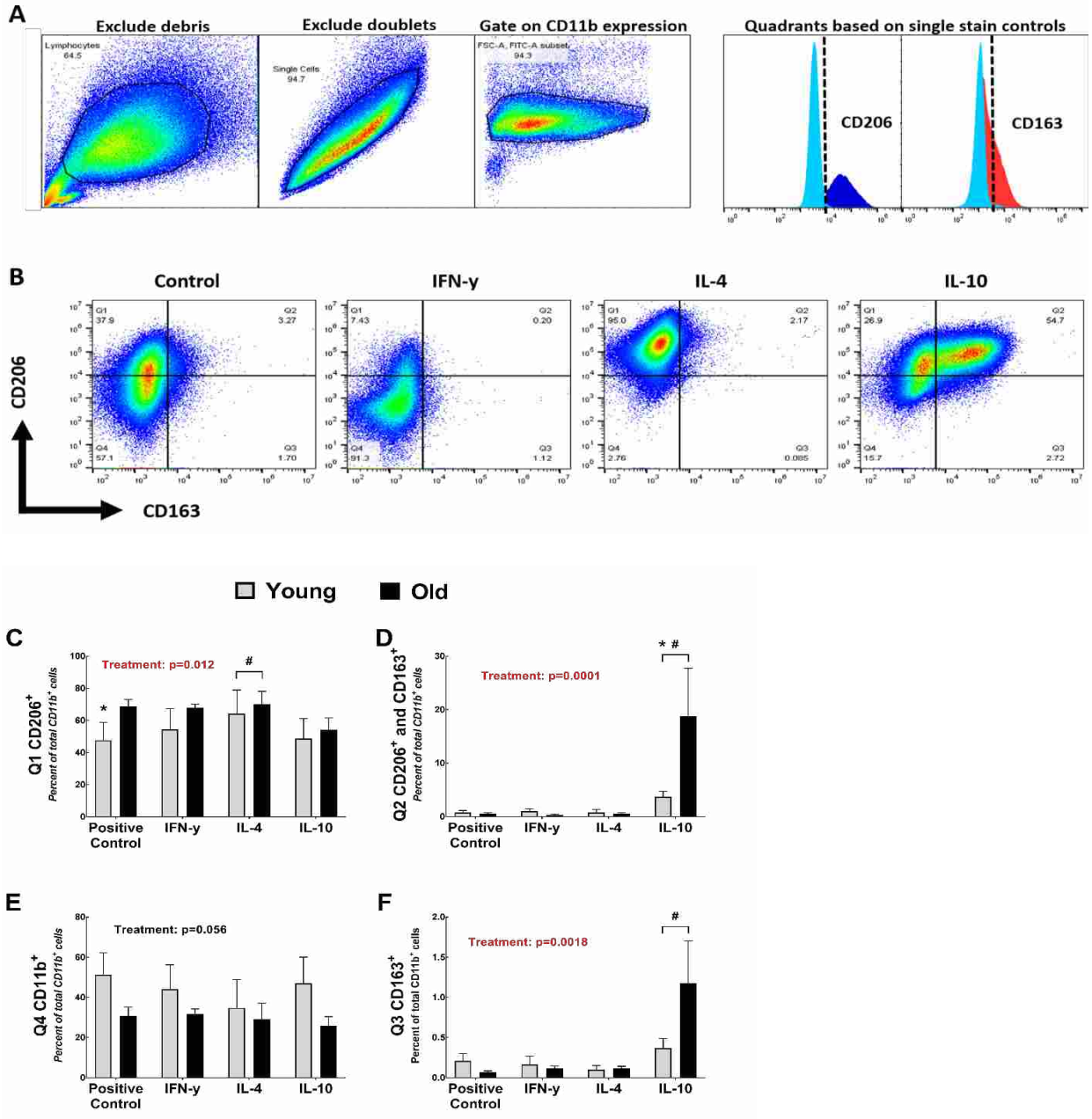

Figure 2.6: Expression of Cell Surface Markers. (A) 350,000 events per sample were gated to display all single macrophages expressing CD11b (pan macrophage marker used in flow cytometry) then further characterized by the expression of **(B)** CD206 and CD163. **(C)** Macrophages that were positive for CD206, **(D)** CD206 and CD163, **(E)** CD11b and **(F)** CD163. Data are presented as means ± SEM. All data are presented as a proportion of total CD11b macrophages. #Significant treatment effect. *Significant difference between young and old. Significance set at $p < 0.05$.

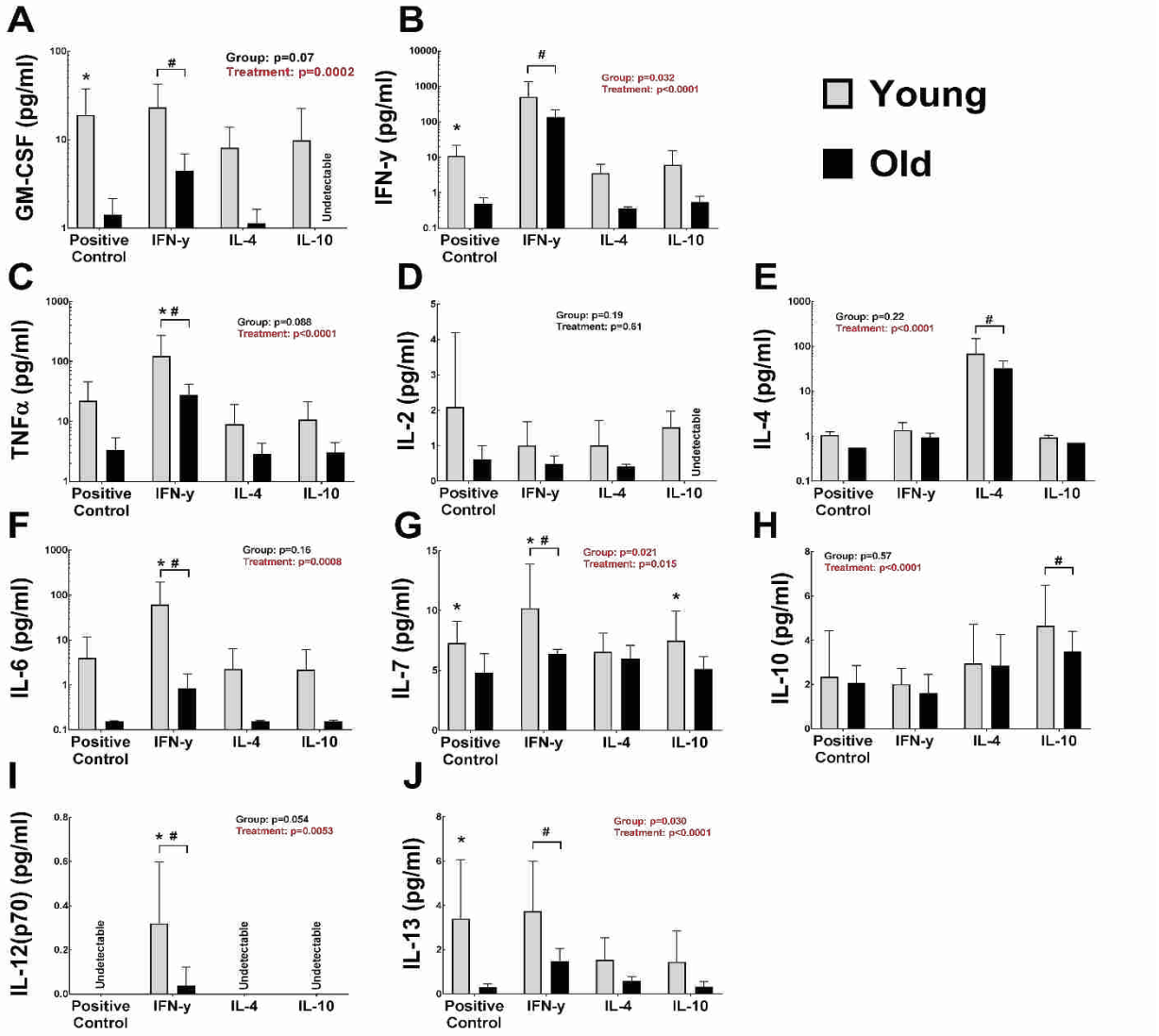

Figure 2.7: Cytokine Concentrations. Conditioned medium was tested for cytokine content of **(A)** GM-CSF, **(B)** IFN-γ, **(C)** TNFα, **(D)** IL-2, **(E)** IL-4, **(F)** IL-6, **(G)** IL-7, **(H)** IL-10, **(I)** IL-12(p40), **(J)** IL-13 using a 13-panel multiplexed magnetic bead assay following 48 hours of incubation with macrophages treated to induce a proinflammatory or anti-inflammatory phenotype. Data are means ± SEM for 10 detectable cytokines. Cytokines were deemed undetectable when the majority of the observations were outside the standard detection limits. The minimum detection limit ranged from 0.14 to 1.12 pg/mL. The 2 undetectable cytokines that did not meet the minimum detection limit were: IL-1b and IL-5. The cytokine that was above the detectable range was IL-8. #Significant treatment effect. *Significant difference between young and old. Significance set at $p < 0.05$.

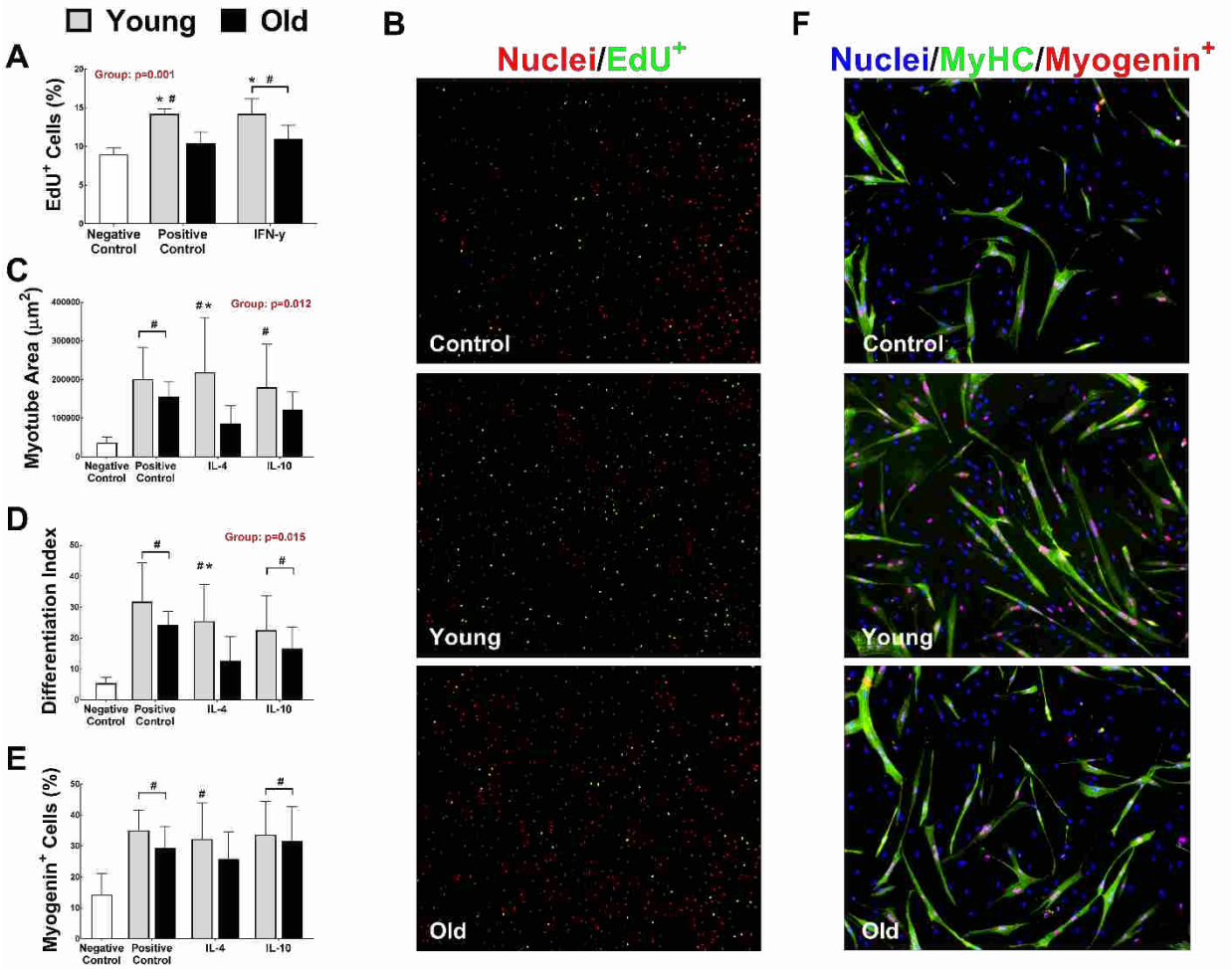

Figure 2.8: Aged Myoblasts in Macrophage-Conditioned Medium. (A) Proliferation of old human primary myoblasts was assessed by the expression of EdU^+ cells following 24 hours in young macrophage-conditioned and old macrophage-conditioned medium or an untreated control with **(B)** representative images (red) nuclei and (green) EdU^+ cells. Differentiation was measured by the development of myotubes using **(C)** myosin heavy chain (MyHC) expression and the **(D)** differentiation index ($MyHC^+$ nuclei/total nuclei). **(E)** Percentage of $myogenin^+$ nuclei/total nuclei. (F) Representative images: (blue) nuclei, (green) myosin heavy chain, and (red) $myogenin^+$ nuclei. Data are means ± SEM. #Significantly different from untreated medium. *Significant difference between young and old. Significance set at $p < 0.05$.

REFERENCES

1. Stewart KJ. Physical activity and aging. Annals of the New York Academy of Sciences. 2005;1055(1):193-206.
2. Sylvia I, Watkins-Castillo SW, Yelin E. United States Bone and Joint Initiative: The Burden of Musculoskeletal Diseases in the United States (BMUS) http://www.boneandjointburden.org/ [updated 2017].
3. Hu X, Ivashkiv LB. Cross-regulation of signaling pathways by interferon-gamma: implications for immune responses and autoimmune diseases. Immunity. 2009;31(4):539-50.
4. Antunes AC, Araujo DA, Verissimo MT, Amaral TF. Sarcopenia and hospitalisation costs in older adults: a cross-sectional study. Nutrition and Dietetics . 2017;74(1):46-50.
5. Janssen I, Shepard DS, Katzmarzyk PT, Roubenoff R. The healthcare costs of sarcopenia in the United States. Journal of the American Geriatrics Society. 2004;52(1):80-5.
6. Sousa AS, Guerra RS, Fonseca I, Pichel F, Ferreira S, Amaral TF. Financial impact of sarcopenia on hospitalization costs. European Journal of Clinical Nutrition. 2016;70(9):1046-51.
7. Murphy MM, Lawson JA, Mathew SJ, Hutcheson DA, Kardon G. Satellite cells, connective tissue fibroblasts and their interactions are crucial for muscle regeneration. Development. 2011;138(17):3625-37.
8. Tidball JG. Regulation of muscle growth and regeneration by the immune system. Nature Reviews Immunology. 2017;17(3):165-78.
9. Saclier M, Yacoub-Youssef H, Mackey AL, Arnold L, Ardjoune H, Magnan M, et al. Differentially activated macrophages orchestrate myogenic precursor cell fate during human skeletal muscle regeneration. Stem Cells. 2013;31(2):384-96.
10. Shireman PK, Contreras-Shannon V, Ochoa O, Karia BP, Michalek JE, McManus LM. MCP-1 deficiency causes altered inflammation with impaired skeletal muscle regeneration. Journal of Leukocyte Biology. 2007;81(3):775-85.
11. Lemos DR, Babaeijandaghi F, Low M, Chang CK, Lee ST, Fiore D, et al. Nilotinib reduces muscle fibrosis in chronic muscle injury by promoting TNF-mediated apoptosis of fibro/adipogenic progenitors. Nature Medicine. 2015;21(7):786-94.
12. Linehan E, Fitzgerald D. Ageing and the immune system: focus on macrophages. European Journal of Microbiology and Immunology. 2015;5(1):14-24.
13. Przybyla B, Gurley C, Harvey JF, Bearden E, Kortebein P, Evans WJ, et al. Aging alters macrophage properties in human skeletal muscle both at rest and in response to acute resistance exercise. Experimental Gerontology. 2006;41(3):320-7.
14. Sorensen JR, Skousen C, Holland A, Williams K, Hyldahl RD. Acute extracellular matrix, inflammatory and MAPK response to lengthening contractions in elderly human skeletal muscle. Experimental Gerontology. 2018;106:28-38.
15. Deyhle MR, Sorensen JR, Hyldahl RD. Induction and assessment of exertional skeletal muscle damage in humans. Journal of Visualized Experiments: JoVE. 2016(118).
16. Deyhle MR, Gier AM, Evans KC, Eggett DL, Nelson WB, Parcell AC, et al. Skeletal muscle inflammation following repeated bouts of lengthening contractions in humans. Frontiers in Physiology. 2015;6:424.
17. Wang Y, Wehling-Henricks M, Samengo G, Tidball JG. Increases of M2a macrophages and fibrosis in aging muscle are influenced by bone marrow aging and negatively regulated by musclederived nitric oxide. Aging Cell. 2015;14(4):678-88.

18. Rebo J, Mehdipour M, Gathwala R, Causey K, Liu Y, Conboy MJ, et al. A single heterochronic blood exchange reveals rapid inhibition of multiple tissues by old blood. Nature Communications. 2016;7:13363.
19. Wang Y, Wehling-Henricks M, Welc SS, Fisher AL, Zuo Q, Tidball JG. Aging of the immune system causes reductions in muscle stem cell populations, promotes their shift to a fibrogenic phenotype, and modulates sarcopenia. FASEB Journal. 2018:fj201800973R.
20. Menck K, Behme D, Pantke M, Reiling N, Binder C, Pukrop T, et al. Isolation of human monocytes by double gradient centrifugation and their differentiation to macrophages in teflon-coated cell culture bags. Journal of Visualized Experiments: JoVE. 2014(91).
21. Agley CC, Rowlerson AM, Velloso CP, Lazarus NL, Harridge SD. Isolation and quantitative immunocytochemical characterization of primary myogenic cells and fibroblasts from human skeletal muscle. Journal of Visualized Experiments : JoVE. 2015(95):52049.
22. Renault V, Thornell LE, Eriksson PO, Butler-Browne G, Mouly V. Regenerative potential of human skeletal muscle during aging. Aging Cell. 2002;1(2):132-9.
23. Carlson ME, Suetta C, Conboy MJ, Aagaard P, Mackey A, Kjaer M, et al. Molecular aging and rejuvenation of human muscle stem cells. EMBO Molecular Medicine. 2009;1(8-9):381-91.
24. Kuswanto W, Burzyn D, Panduro M, Wang KK, Jang YC, Wagers AJ, et al. Poor repair of skeletal muscle in aging mice reflects a defect in local, interleukin-33-dependent accumulation of regulatory T cells. Immunity. 2016;44(2):355-67.
25. Tidball JG, Villalta SA. Regulatory interactions between muscle and the immune system during muscle regeneration. American Journal of Physiology Regulatory, Integrative and Comparative Physiology. 2010;298(5):R1173-87.
26. Calve S, Odelberg SJ, Simon HG. A transitional extracellular matrix instructs cell behavior during muscle regeneration. Developmental Biology. 2010;344(1):259-71.
27. Murphy MM, Lawson JA, Mathew SJ, Hutcheson DA, Kardon G. Satellite cells, connective tissue fibroblasts and their interactions are crucial for muscle regeneration. Development. 2011;138(17):3625-37.
28. Bernet JD, Doles JD, Hall JK, Kelly Tanaka K, Carter TA, Olwin BB. p38 MAPK signaling underlies a cell-autonomous loss of stem cell self-renewal in skeletal muscle of aged mice. Nature Medicine. 2014;20(3):265-71.
29. Peake JM, Neubauer O, Della Gatta PA, Nosaka K. Muscle damage and inflammation during recovery from exercise. Journal of Applied Physiology. 2017;122(3):559-70.
30. Hyldahl RD, Nelson B, Xin L, Welling T, Groscost L, Hubal MJ, et al. Extracellular matrix remodeling and its contribution to protective adaptation following lengthening contractions in human muscle. FASEB Journal. 2015;29(7):2894-904.
31. Biernacka A, Frangogiannis NG. Aging and cardiac fibrosis. Aging and Disease. 2011;2(2):158-73.
32. Leung J, Cho Y, Lockey RF, Kolliputi N. The role of aging in idiopathic pulmonary fibrosis. Lung. 2015;193(4):605-10.
33. Van Thienen R, D'Hulst G, Deldicque L, Hespel P. Biochemical artifacts in experiments involving repeated biopsies in the same muscle. Physiological Reports. 2014;2(5):e00286.
34. Jennekens F, Tomlinson B, Walton J. Data on the distribution of fibre types in five human limb muscles An autopsy study. Journal of the Neurological Sciences. 1971;14(3):245-57.
35. Ramsey F, Schafer D. The statistical sleuth: a course in methods of data analysis: Cengage Learning; 2012.

36. Peake J, Della Gatta P, Cameron-Smith D. Aging and its effects on inflammation in skeletal muscle at rest and following exercise-induced muscle injury. American Journal of Physiology Regulatory, Integrative and Comparative Physiology. 2010;298(6):R1485-95.
37. Gosselin LE, Adams C, Cotter TA, McCormick RJ, Thomas DP. Effect of exercise training on passive stiffness in locomotor skeletal muscle: role of extracellular matrix. Journal of Applied Physiology. 1998;85(3):1011-6.
38. Chodzko-Zajko WJ, Proctor DN, Singh MAF, Minson CT, Nigg CR, Salem GJ, et al. Exercise and physical activity for older adults. Medicine & Science in Sports & Exercise. 2009;41(7):1510-30.
39. Verdijk LB, Koopman R, Schaart G, Meijer K, Savelberg HH, van Loon LJ. Satellite cell content is specifically reduced in type II skeletal muscle fibers in the elderly. American Journal of Physiology-Endocrinology and Metabolism. 2007;292(1):E151-E7.
40. Evans WJ, Lexell J. Human aging, muscle mass, and fiber type composition. The Journals of Gerontology Series A: Biological Sciences and Medical Sciences. 1995;50(Special Issue):11-6.
41. Paulsen G, Mikkelsen UR, Raastad T, Peake JM. Leucocytes, cytokines and satellite cells: what role do they play in muscle damage and regeneration following eccentric exercise? Exercise Immunology Review. 2012;18:42-97.
42. Lavender AP, Nosaka K. Comparison between old and young men for changes in makers of muscle damage following voluntary eccentric exercise of the elbow flexors. Applied Physiology, Nutrition, and Metabolism. 2006;31(3):218-25.
43. Manfredi TG, Fielding RA, O'Reilly KP, Meredith CN, Lee HY, Evans WJ. Plasma creatine kinase activity and exercise-induced muscle damage in older men. Medicine & Science in Sports & Exercise. 1991;23(9):1028-34.
44. Callahan DM, Kent-Braun JA. Effect of old age on human skeletal muscle force-velocity and fatigue properties. Journal of Applied Physiology (1985). 2011;111(5):1345-52.
45. Hortobagyi T, Zheng D, Weidner M, Lambert NJ, Westbrook S, Houmard JA. The influence of aging on muscle strength and muscle fiber characteristics with special reference to eccentric strength. The Journals of Gerontology Series A, Biological Sciences and Medical Sciences. 1995;50(6):B399-406.
46. Roig M, Macintyre DL, Eng JJ, Narici MV, Maganaris CN, Reid WD. Preservation of eccentric strength in older adults: evidence, mechanisms and implications for training and rehabilitation. Experimental Gerontology. 2010;45(6):400-9.
47. Mackey AL, Brandstetter S, Schjerling P, Bojsen-Moller J, Qvortrup K, Pedersen MM, et al. Sequenced response of extracellular matrix deadhesion and fibrotic regulators after muscle damage is involved in protection against future injury in human skeletal muscle. FASEB Journal. 2011;25(6):1943-59.
48. Tierney MT, Gromova A, Sesillo FB, Sala D, Spenle C, Orend G, et al. Autonomous extracellular matrix remodeling controls a progressive adaptation in muscle stem cell regenerative capacity during development. Cell Reports. 2016;14(8):1940-52.
49. Grounds MD. Age-associated changes in the response of skeletal muscle cells to exercise and regeneration. Annals of the New York Academy of Sciences. 1998;854:78-91.
50. Merritt EK, Stec MJ, Thalacker-Mercer A, Windham ST, Cross JM, Shelley DP, et al. Heightened muscle inflammation susceptibility may impair regenerative capacity in aging humans. Journal of Applied Physiology. 2013;115(6):937-48.

51. Peake JM, Della Gatta P, Suzuki K, Nieman DC. Cytokine expression and secretion by skeletal muscle cells: regulatory mechanisms and exercise effects. Exercise Immunology Review. 2015;21:8-25.
52. Moore LB, Sawyer AJ, Charokopos A, Skokos EA, Kyriakides TR. Loss of monocyte chemoattractant protein-1 alters macrophage polarization and reduces NFkB activation in the foreign body response. Acta Biomaterialia. 2015;11:37-47.
53. Villalta SA, Nguyen HX, Deng B, Gotoh T, Tidball JG. Shifts in macrophage phenotypes and macrophage competition for arginine metabolism affect the severity of muscle pathology in muscular dystrophy. Human Molecular Genetics. 2009;18(3):482-96.
54. Li Y-P, Chen Y, John J, Moylan J, Jin B, Mann DL, et al. TNF-α acts via p38 MAPK to stimulate expression of the ubiquitin ligase atrogin1/MAFbx in skeletal muscle. FASEB Journal. 2005;19(3):362-70.
55. Williamson D, Gallagher P, Harber M, Hollon C, Trappe S. Mitogen-activated protein kinase (MAPK) pathway activation: effects of age and acute exercise on human skeletal muscle. The Journal of Physiology. 2003;547(3):977-87.
56. Roux PP, Blenis J. ERK and p38 MAPK-activated protein kinases: a family of protein kinases with diverse biological functions. Microbiology and Molecular Biology Reviews. 2004;68(2):320-44.
57. Pogozelski AR, Geng T, Li P, Yin X, Lira VA, Zhang M, et al. p38γ mitogen-activated protein kinase is a key regulator in skeletal muscle metabolic adaptation in mice. PloS One. 2009;4(11):e7934.
58. Perdiguero E, Sousa-Victor P, Ruiz-Bonilla V, Jardi M, Caelles C, Serrano AL, et al. p38/MKP-1-regulated AKT coordinates macrophage transitions and resolution of inflammation during tissue repair. Cell Biology. 2011;195(2):307-22.
59. Troy A, Cadwallader AB, Fedorov Y, Tyner K, Tanaka KK, Olwin BB. Coordination of satellite cell activation and self-renewal by Par-complex-dependent asymmetric activation of p38α/β MAPK. Cell Stem Cell. 2012;11(4):541-53.
60. Keefe AC, Lawson JA, Flygare SD, Fox ZD, Colasanto MP, Mathew SJ, et al. Muscle stem cells contribute to myofibres in sedentary adult mice. Nature Communications. 2015;6.
61. Hall JK, Banks GB, Chamberlain JS, Olwin BB. Prevention of muscle aging by myofiber-associated satellite cell transplantation. Science Translational Medicine. 2010;2(57):57ra83.
62. Conboy IM, Conboy MJ, Wagers AJ, Girma ER, Weissman IL, Rando TA. Rejuvenation of aged progenitor cells by exposure to a young systemic environment. Nature. 2005;433(7027):760-4.
63. Carlson B, Faulkner J. Muscle transplantation between young and old rats: age of host determines recovery. American Journal of Physiology-Cell Physiology. 1989;256(6):C1262-C6.
64. Davies LC, Jenkins SJ, Allen JE, Taylor PR. Tissue-resident macrophages. Nature Immunology. 2013;14(10):986-95.
65. Arnold L, Henry A, Poron F, Baba-Amer Y, Van Rooijen N, Plonquet A, et al. Inflammatory monocytes recruited after skeletal muscle injury switch into anti-inflammatory macrophages to support myogenesis. Experimental Medicine. 2007;204(5):1057-69.
66. Valentin JE, Stewart-Akers AM, Gilbert TW, Badylak SF. Macrophage participation in the degradation and remodeling of extracellular matrix scaffolds. Tissue Engineering Part A. 2009;15(7):1687-94.

67. Alexakis C, Partridge T, Bou-Gharios G. Implication of the satellite cell in dystrophic muscle fibrosis: a self-perpetuating mechanism of collagen overproduction. American Journal of Physiology-Cell Physiology. 2007;293(2):C661-C9.
68. Villalta SA, Deng B, Rinaldi C, Wehling-Henricks M, Tidball JG. IFN-gamma promotes muscle damage in the mdx mouse model of Duchenne muscular dystrophy by suppressing M2 macrophage activation and inhibiting muscle cell proliferation. Immunology. 2011;187(10):5419-28.
69. Ruffell D, Mourkioti F, Gambardella A, Kirstetter P, Lopez RG, Rosenthal N, et al. A CREB-C/EBPbeta cascade induces M2 macrophage-specific gene expression and promotes muscle injury repair. Proceedings of the National Academy of Sciences of the United States of America. 2009;106(41):17475-80.
70. Mann CJ, Perdiguero E, Kharraz Y, Aguilar S, Pessina P, Serrano AL, et al. Aberrant repair and fibrosis development in skeletal muscle. Skeletal Muscle. 2011;1(1):21.
71. Heppner HJ, Cornel S, Peter W, Philipp B, Katrin S. Infections in the elderly. Critical Care Clinics. 2013;29(3):757-74.
72. Aspinall R, Del Giudice G, Effros RB, Grubeck-Loebenstein B, Sambhara S. Challenges for vaccination in the elderly. Immunity & Ageing. 2007;4(1):9.
73. Katz JM, Plowden J, Renshaw-Hoelscher M, Lu X, Tumpey TM, Sambhara S. Immunity to influenza: the challenges of protecting an aging population. Immunologic Research. 2004;29(1-3):113-24.
74. Reidy PT, Lindsay CC, McKenzie AI, Fry CS, Supiano MA, Marcus RL, et al. Aging-related effects of bed rest followed by eccentric exercise rehabilitation on skeletal muscle macrophages and insulin sensitivity. Experimental Gerontology. 2017.
75. Brigitte M, Schilte C, Plonquet A, Baba-Amer Y, Henri A, Charlier C, et al. Muscle resident macrophages control the immune cell reaction in a mouse model of notexin-induced myoinjury. Arthritis & Rheumatology. 2010;62(1):268-79.
76. Shireman PK, Contreras‐Shannon V, Ochoa O, Karia BP, Michalek JE, McManus LM. MCP‐1 deficiency causes altered inflammation with impaired skeletal muscle regeneration. Journal of Leukocyte Biology. 2007;81(3):775-85.
77. Herrero C, Marques L, Lloberas J, Celada A. IFN-gamma-dependent transcription of MHC class II IA is impaired in macrophages from aged mice. The Journal of Clinical Investigation. 2001;107(4):485-93.
78. Reidy PT, Lindsay CC, McKenzie AI, Fry CS, Supiano MA, Marcus RL, et al. Aging-related effects of bed rest followed by eccentric exercise rehabilitation on skeletal muscle macrophages and insulin sensitivity. Experimental Gerontology. 2017.
79. Londhe P, Davie JK. Gamma interferon modulates myogenesis through the major histocompatibility complex class II transactivator, CIITA. Molecular Cell Biology. 2011;31(14):2854-66.
80. Deng B, Wehling-Henricks M, Villalta SA, Wang Y, Tidball JG. IL-10 triggers changes in macrophage phenotype that promote muscle growth and regeneration. Immunology. 2012:1103180.
81. Pizza FX, Peterson JM, Baas JH, Koh TJ. Neutrophils contribute to muscle injury and impair its resolution after lengthening contractions in mice. The Journal of Physiology. 2005;562(3):899-913.

82. Lockhart NC, Brooks SV. Neutrophil accumulation following passive stretches contributes to adaptations that reduce contraction-induced skeletal muscle injury in mice. Journal of Applied Physiology. 2008;104(4):1109-15.
83. Sloboda DD, Brown LA, Brooks SV. Myeloid cell responses to contraction-induced injury differ in muscles of young and old mice. The Journals of Gerontology Series A, Biological Sciences and Medical Sciences. 2018.
84. Van den Bossche J, Baardman J, de Winther MP. Metabolic characterization of polarized M1 and M2 bone marrow-derived macrophages using real-time extracellular flux analysis. Journal of Visualized Experiments: JoVE. 2015(105).
85. Mahbub S, Deburghgraeve CR, Kovacs EJ. Advanced age impairs macrophage polarization. Journal of Interferon & Cytokine Research: the Official Journal of the International Society for Interferon and Cytokine Research. 2012;32(1):18-26.
86. Akahori H, Karmali V, Polavarapu R, Lyle AN, Weiss D, Shin E, et al. CD163 Interacts with TWEAK to regulate tissue regeneration after ischaemic injury. Nature Communications. 2015;6:7792.